Effect of microstructure on shear strength and dilatancy of unsaturated loess at high suctions

Author's affiliation and address:

Name: Charles Wang Wai Ng
Affiliation: CLP Holdings Professor of Sustainability
Address: Department of Civil and Environmental Engineering, Hong Kong University of Science and Technology, Clear Water Bay, Kowloon, Hong Kong
E-mail: cecwwng@ust.hk

Name: Hamed Sadeghi* (Corresponding author)
Affiliation: Assistant Professor
Address: Department of Civil Engineering, Sharif University of Technology, Tehran, Iran
E-mail: hsadeghi@sharif.edu

Name: Fardin Jafarzadeh
Affiliation: Associate Professor
Address: Department of Civil Engineering, Sharif University of Technology, Tehran, Iran
E-mail: fardin@sharif.edu

Name: Mohammad Sadeghi
Affiliation: Graduate Research Assistant
Address: Department of Civil Engineering, Sharif University of Technology, Tehran, Iran
E-mail: mhmd.sadeghi@gmail.com

Name: Chao Zhou
Affiliation: Assistant Professor
Address: Department of Civil and Environmental Engineering, The Hong Kong Polytechnic University, Hung Hom, Hong Kong
E-mail: c.zhou@polyu.edu.hk

Name: Sina Baghbanrezvan
Affiliation: PhD Student
Address: Department of Civil and Environmental Engineering, Hong Kong University of Science and Technology, Clear Water Bay, Kowloon, Hong Kong
E-mail: sbad@connect.ust.hk

ABSTRACT

In order to investigate the influences of microstructure changes on dilatancy of unsaturated loess at high suctions, a direct shear box device using the vapour equilibrium technique was used. Through conducting two series of direct shear tests on both intact and recompacted loess specimens and also investigating microstructural changes using the Mercury Intrusion Porosimetry (MIP) technique, a linear increase in dilatancy with suction ranging from 8 to 230 MPa can be identified at different net stresses. The enhanced dilatancy observed is mainly attributed to desiccation-induced high suctions since the reduction in void ratio due to enhancement of suction was negligible. A macrovoid ratio, e_M, may be quantified and proposed to explain the differences in the increased dilatancy of recompacted and intact loess with suction.

KEYWORDS: loess; microstructure; dilatancy; high suction; void ratio

INTRODUCTION

It is well understood that dilatancy plays a major role in governing shear behaviour of saturated soils. Taylor (1948) revealed the contribution of density on dilatancy and strength of soils. After his pioneer work, Rowe (1962) presented his theory on stress-dilatancy followed by Bolton (1986) whose main contribution was introducing a new relative density index. The advancement of knowledge and understanding of unsaturated soil behaviour revealed that in addition to net stress, suction is considered as another stress state variable affecting mechanical behaviour and dilation (Alonso et al. 1990; Wheeler and Sivakumar 1995; Cui and Delage 1996; Ng and Chiu 2003; Chávez and Alonso 2003; Ng and Zhou 2005; Alonso et al. 2007). Cui and Delage (1996) reported a series of triaxial test results on compacted silt, indicating a clear enhancement of dilation rate by suction. Chiu and Ng (2003) introduced a state-dependent elasto-plastic model in which the original state parameter of Been and Jefferies (1985) was considered as a function of

suction. Suction-dependent dilatancy was later supported by experimental results of Chávez and Alonso (2003); Ng and Zhou (2005) and Alonso et al. (2007) for other types of geomaterials.

Most of these studies were conducted on unsaturated compacted fine-grained soils, whereas, previous studies on unsaturated loess, characterised as an aeolian, open structure soil, were focused on collapse behaviour and water retention properties. Munoz-Castelblanco et al. (2011) investigated collapse behaviour of an unsaturated intact loess. It was concluded that collapse of large constricted macropores was responsible for significant volumetric plastic strain upon soaking at constant vertical stress. Munoz-Castelblanco et al. (2012) extended their study by looking into water retention characteristics of natural undisturbed loess. No hysteresis was observed around the *in-situ* water content, with two hysteresis loops on the dry and wet sides with reference to the *in-situ* water content. It was hypothesised no hysteresis around the *in-situ* water content could be corresponding to the seasonal variations in water content.

Natural loess with an aeolian geological origin is characterised by relatively high void ratio and sustains a meta-stable structure provided by inter-particle suction reinforcement under unsaturated conditions (Munoz-Castelblanco et al. 2012; Ng et al. 2016). Although the significant role of microstructure on compressibility (Munoz-Castelblanco et al. 2011), collapse behaviour (Haeri et al. 2014) and water retention characteristics of loess (Munoz-Castelblanco et al. 2012; Ng et al. 2016) has been highlighted, less effort has been put forward to clarify the significance of microstructure on shear strength and dilatancy. In other words, in most of studies focused on shear behaviour of loess, microstructure was not measured and its effects were not analysed. For example, the compression and shear strength characteristics of unsaturated recompacted loess were investigated by Ng et al. (2017b), but the effects of different microstructures resulting from natural forming process and artificial recompaction were ignored in their study.

There have been limited number of studies so far to compare the shear behaviour of intact and recompacted loess. Wen and Yan (2014) compared shear strength of unsaturated undisturbed,

and remoulded loess. Their test specimens were brought to a specific degree of saturation by air drying or adding distilled water onto them. Accordingly, shear strength was evaluated by using a conventional direct shear box and the corresponding suction was inferred from the results of pressure plate tests. In other words, suction was neither controlled nor measured in the shear box. In addition, test specimens were sheared under unconsolidated undrained condition with a high shearing rate of 14 mm/min. Comparison of test results between undisturbed and remoulded loess revealed that the peak shear strength significantly reduced due to the destruction of natural bonding of undisturbed loess by remoulding it. However, soil volume changes during shearing were not measured. Effects of suction and microstructure on dilatancy, being the main focus of the current study, were not investigated. On the contrary, Haeri et al. (2016) reported higher shear strength for recompacted loess than that of intact loess at the same matric suction and net stress. They carried out their tests at low suctions ranging from zero to 400 kPa and they suggested that the difference in shear strength was attributed to the non-homogeneous distribution of pores in intact loess. However, the microstructural states of intact and recompacted specimens were not quantified.

Field monitoring of relative humidity (*RH*) during year 2012 in Xi′an, China where the intact block samples were retrieved, proved the variations in *RH* ranging from 45% to 85%, typically (Sadeghi 2016). It is interesting to note that the axis translation technique considered as the most common suction control method in laboratory testing is limited to an *RH* as high as 98.9% even though a 15-bar high air entry disk be utilized. Therefore, the most common current practice may not be suitable for simulating the *in-situ* soil conditions in laboratory. More important, results of suction measurements on block samples revealed an inverse suction profile varied from 70 kPa to 40 MPa at depths of 1.5 m and 7.5 m, respectively (Ng et al. 2017a). The main reason was the deep groundwater table beyond 60 m and a recent irrigation prior to sampling. The occurrence of deep groundwater table in loess stratum in semi-arid to arid regions was also reported for the loess in Southeast of Iran (Sadeghi et al. 2019). Indeed, deep monitoring of

suction is inevitable in such cases (Sadeghi et al. 2018). Therefore, the practical implication of considering high suction and enhanced dilation in studying loess behaviour is to coming out with a more reliable and rational design specifications dictated by the *in-situ* soil conditions. In addition, rainfall infiltration in vadose zone is directly governed by permeability of water phase. Field measurements revealed that a significant reduction in permeability function about two to three order of magnitudes can readily happen due to the enhancement of suction (Ng et al. 2011). This will in turn affect shear strength properties and hence the nature of slope instability. There is no need to mention that dilation has a direct influence on peak shear strength. Accordingly, reliable evaluation of shear strength parameters results in a better understanding of natural soil behaviour as well as a more economic design of geostructures in such soils (e.g. Li et al. 2016) where the near saturation conditions are very unlikely to happen.

The main objective of this study is to explore the effects of microstructure on dilatancy of unsaturated loess at high suctions, in particular. It is also aimed to examine the effectiveness of void ratio for precise description of shear behaviour when microstructure of soil changes. In this study, results of two series of saturated and unsaturated tests on recompacted and intact loess using a humidity controlled direct shear apparatus are reported and discussed. Moreover, MIP examinations are carried out to investigate the influence of microstructure changes on dilatancy.

LABORATORY PROCEDURES

Soil type and specimen preparation

Block samples were extracted manually from an excavated pit for sampling purpose in Xi'an, Shaanxi Province of China. They were obtained from four different depths, starting from 1.5 m to 7.5 m at 2 m intervals. Retrieved cubic block samples with 0.25-m-long sides were immediately covered with a plastic membrane and then wrapped in several cloth-paraffin wax

isolation layers to minimize water loss. These samples were fitted into slightly bigger rigid wooden boxes with Styrofoam inner walls. Water contents of some selected samples were also measured on site. All block samples were thereafter delivered from Xi′an to Hong Kong by air freight to minimize transportation time. Prior to testing the delivered block samples, water contents were determined and compared to those measured on site. A very little difference of 0.2% was found. Loess contains 0.1%, 71.9%, and 28.0% of sand, silt, and clay particles, respectively. The specific gravity, plastic limit, and liquid limit were also measured as 2.69, 19%, and 36%, respectively. The soil is classified as a clay of low plasticity according to the Unified Soil Classification System (ASTM 2011a, D 2487). Although silt-size particles are dominating the clay-size particles in the loess, the Atterberg limits of tested loess fall within the zone of lean clay on the plasticity chart. In addition, the loess is classified as a clayey loess according to the zonation proposed by Gibbs and Holland (1960) for categorising three types of loess.

Recompacted specimens were prepared at the target dry density similar to the undisturbed soil. Preliminary measurements on eight samples from different depths showed an average dry density of 1282 kg/m^3. The standard deviation and coefficient of variation of *in-situ* dry densities are 0.05 and 4.2%, respectively, suggesting that the dry densities of the intact specimens have close values to the mean value of dry density. However, the gravimetric water content ranged from 5% to 13% with varying depth. The target water content of 12% corresponding to a depth of 3.5 m was chosen for recompacted tests, since intact specimens at this depth were used.

Results of a series of compaction tests with standard Proctor effort gave maximum dry density and optimum water content of 1680 kg/m^3 and 18.1%, respectively. Therefore, the average state of recompacted specimens in the compaction plane falls on the dry side of optimum water content with a relative compaction (*RC*) of 76%. It is noted that *RC* is defined as the ratio between the current dry density and the maximum one obtained from the standard Proctor test.

Relative compaction is selected and used in this study as a state index since e_{min}, e_{max}, relative density and hence relative dilatancy index (Bolton 1986) can be only determined for coarse-grained soils (ASTM 2011b, D 4253; ASTM 2011c, D 4254). Wet soil was prepared by first spraying the 500 g of oven-dried, sieved and disaggregated soil with the target water content (considering evaporation). It was then kneaded and passed through a 2-mm aperture sieve. This procedure was repeated until no mixture remained on the sieve. Afterwards, the soil was sealed in a zipped plastic bag and kept inside an ice chest for moisture equalisation overnight. Recompacted specimens were statically compacted in three layers at the displacement rate of 1 mm/min inside a three-piece detachable mould. Compaction of the specimen in only one layer would result in density variations along the specimen height. To minimize the variations of soil density, all specimens in this study were prepared in three layers according to ASTM (2000) D 6528. The interface between layers was scarified before compaction of the subsequent layer. It should be pointed out that the shear zone might progressively intercept the weaker layers resulted from compaction procedure. However, the strains and stresses within the final failure zone would be uniform (Potts et al. 1987). In addition, all the specimens were sheared along their mid-height and hence shear plane did not pass through the interface layers. Although the existence of the weak layers may reduce shear strength and dilantancy of the recompacted specimens, the results of this study show that recompacted specimens behave more dilative than the intact ones at high suctions. Consequently, the existence of potential weak layers should not affect the major conclusions drawn from this research. The specimens had the dimensions of 50.8 mm × 50.8 mm × 24.4 mm. Their weight and dimensions were measured after preparation and their water content was determined.

All the intact specimens were taken from a depth of 3.5 m to minimize the natural variability of void ratio, water content and suction with depth and to enable consistent comparisons. In order to prepare a test specimen, an appropriate volume of soil was first cut from a block sample and trimmed to just above the target dimensions. The intact specimens were prepared according to

ASTM (2000) D 6528. Following the extrusion of the specimen from the mould, top and bottom of the specimen were levelled off. The fully trimmed specimen was gently inserted on a sample base. The test specimen was weighed and the trimmed portion of soil was used for water content measurements. In addition, initial suction was measured for two representative specimens of each type (recompacted and intact) using a small-tip tensiometer. Measurements revealed that recompacted and intact loess specimens have the initial suction of 62 kPa and 76 kPa, respectively.

Figs 1(a) and 1(b) indicate soil water retention data in terms of variations in degree of saturation and void ratio versus suction, respectively. Results are presented for both recompacted and intact loess at high suctions measured by vapour equilibrium technique. In spite of significant influence of suction on variations in degree of saturation, void ratio is not significantly influenced by changes in suction at high range. According to Fig. 1(c), no significant difference can be seen between the two sets of measurements at high range of suction in spite of previous observations for low range. Differences in water retention characteristics of recompacted and intact loess were presented and discussed by Ng et al. (2016). Results presented in Fig. 1(c) are used to infer macrovoid ratio (e_M) and microvoid ratio (e_m) for intact and recompacted loess. In order to achieve that, the proposal put forward by Alonso et al. (2013) is used for inferring the microvoid ratio and hence macrovoid ratio from the microstructural parameter, ξ_m, according to Eq. 1:

$$e_m = \xi_m e \quad (1a)$$

$$e_M = e - e_m \quad (1b)$$

It should be also noted that ξ_m equals to the microstructural degree of saturation, S_r^m, corresponding to the residual suction. The microstructural degree of saturation corresponds to the water filling all the microvoids while the macrovoids are completely dry. In order to obtain S_r^m, the residual suction was first derived by intersecting two lines tangent to the residual branch and main desorption path after the air entry value according to Fig. 1(c). The corresponding

degree of saturation was then obtained following the procedure shown in the figure. The microstructural properties of recompacted and intact loess are given in Table 1. Results on loess microstructure are discussed later.

The VET-based direct shear box device

Fig. 2 shows the modified direct shear box chamber used in this study. The developed setup consists of a suction control and monitoring system in addition to the conventional mechanical loading components. The vapour equilibrium technique (VET) was adopted which is a reliable method of controlling relative humidity (*RH*) and hence suction (under isothermal conditions) in an enclosed system (Blatz et al. 2008). This method of controlling suction was utilized in a modified ring shear apparatus for studying residual shear strength properties at high suction (Merchán et al. 2011). Results revealed a significant influence of suction at high range up to 140 MPa on residual friction angle of desiccated clays. Alsherif and McCartney (2015) equipped a triaxial cell with a gas flow control unit in combination with relative humidity feedback system to achieve a target high total suction in the range of 160 to 320 MPa. Temperature was also controlled in the modified device for studying both temperature and high suction influence on shear behaviour. Nishimura (2016) investigated the effects of suction and shearing rate on shear strength of compacted bentonite. A modified direct shear apparatus was used which can provide a constant relative humidity environment through an *RH* air circulation system. Vapour equilibrium technique was also adopted by Sadeghi et al. (2017) in modification of a direct shear device for testing unsaturated soils at high suction range. Relative humidity can be controlled and suction can be monitored in an isolated shear box chamber put inside a controlled temperature room.

In order to achieve the target *RH*, four types of salt—KNO_3, NaCl, $MgCl_2.6H_2O$, and LiCl—were used. The nominal levels of suction generated by saturated solutions of these salts under room temperature are 8, 40, 125, and 230 MPa. Conventional desiccators were used as ancillary

devices to cope with the main drawback of VET, which is long equilibrium time. Although *RH* and temperature were controlled inside the chamber and not directly measured on the specimens, the principles of controlling suction based on vapour transfer technique ensured the uniqueness of suction both in the chamber and soil specimen after equalisation (Blatz et al. 2008). Since the specimens were initially equalized in a desiccator containing the same saturated salt solution as the one used inside the chamber, the equalisation of suction inside the desiccator ensured that suction imposed inside the chamber was satisfactorily achieved in the specimens as well. Fig. 3(a) shows the equalisation stage for control specimens inside four desiccators containing different saturated salt solutions. The control specimens were prepared similar to those compacted specimens for continuous weighing and checking moisture equalisation. According to the results, the duration for equalisation of suction lasted for two to eight weeks, depending on the target suction level. Afterwards, the test specimens were directly transferred to the chamber with the identical temperature and *RH* conditions to ensure the achievement of target suction satisfactorily.

The environmental conditions inside the shear box chamber were monitored during compression and shearing stages of tests at different suction levels. An EL-USB-2-LCD humidity/temperature data logger manufactured by the Lascar Electronics was used to monitor and record environmental conditions inside the chamber during the tests. The probe covers an *RH* range of zero to 100% with an accuracy of ±3%. Temperature can also be measured with an accuracy of $\pm 0.5^0$C from -35^0C to 80^0C. More details about the apparatus can be found in Sadeghi et al. (2017). Relative humidity and temperature were recorded at 10 min time intervals and suction was evaluated based on the psychometric law. Fig. 3(b) and (c) show the *RH* and temperature measured during compression and shearing stages. No sharp changes in *RH* and temperature were observed during the shearing stage. The standard deviation of measured suction values is less than 1.3 for all the specimens tested, suggesting minimal change in soil

suction. Therefore, a nearly steady state condition can be assumed for suction with negligible fluctuations throughout the whole test.

Stress paths followed in direct shear tests

Two series of saturated and unsaturated tests were carried out on intact and recompacted loess. The corresponding stress paths for saturated and unsaturated tests are illustrated in Figs 4(a) and (b), respectively. Saturated tests were initiated by loading at constant water content (assuming minimum evaporation inside the enclosed chamber) to the target vertical stress along path AB_i in Fig. 4(a) until equilibrium in displacement was reached. Specimens were soaked afterwards (B_iC_i) by injecting water into the chamber and monitoring axial displacements. Once the specimens were consolidated, they were sheared (C_iD_i) at a constant displacement rate of 0.0019 mm/min to ensure drained conditions. In unsaturated tests, specimens were first dried from the initial state to the target suction along path AB_i in Fig. 4(b) inside conventional desiccators. They were then compressed under constant suction to the target net stress following a step loading scheme (B_iC_i). They were eventually sheared at the same rate as that in saturated tests (C_iD_i). Research on effect of shear rate on stress strain behaviour at high suction range is quite rare. Nishimura and Vanapalli (2005) studied this phenomenon and observed a decrease in peak shear strength with shear rate. The minimum rate used in their study was 0.03 %/min. The suitable shear strain rate for unsaturated tests at high suction was investigated recently by Patil et al. (2015). Based on a series of tests at five different shearing rates, it was concluded that the strain rate of 0.0009 %/min is slow enough to have the least influence on peak and critical state in triaxial testing. The proposed strain rate can be converted to a displacement rate of 0.0013 mm/min for the triaxial specimens used (Patil et al. 2016). Therefore, a comparable shear rate of 0.0019 mm/min was also used in this research for both saturated and unsaturated direct shear tests. The adopted stress paths allow studying compressibility, collapse potential as well as shear behaviour of materials tested.

Test programme

The experimental programme for macroscopic behaviour included two series of saturated and unsaturated direct shear tests on intact and recompacted loess. The first series consisted of six saturated tests conducted to investigate collapsibility as well as shear strength characteristics of saturated loess. Tests were conducted at vertical effective stresses of 50, 100, and 200 kPa. Details of saturated tests are summarised in Table 2. The second series of tests included 16 suction-controlled unsaturated tests on intact and recompacted loess (8 for each). Tests were run at four suction levels ranging from 8 to 230 MPa. In addition, the specimens were compressed to two vertical net stresses of 50 and 200 kPa. Testing conditions of all unsaturated tests are detailed in Table 3.

Microstructural investigations

The microstructure of test specimens was investigated at initial state and after suction equalisation through MIP tests. Since MIP devices require dry specimens in addition to the fact that any change in water content would change the soil structure, water was removed via a freeze-drying process. Water dries up in a freeze-dryer through a sublimation mechanism in which the curvature of the water-air interface and hence inter-particle forces would not change. As a result, the structure of soil specimens is preserved after complete drying (Delage et al. 1982). Test specimens were dried in an Edwards Super Modulyo freeze-dryer and tested in a Micromeritics Auto Pore IV 9500 V 1.04 MIP device. Two series of MIP tests were conducted on both intact and recompacted loess. Test conditions will be presented and explained later.

INTERPRETATION OF TEST RESULTS

Volume changes due to constant-load wetting and suction equalisation

Variations in void ratio with different testing stages are shown in Fig. 5(a). Three stages are considered including: (0) initial state, (1) after compressing to a specific normal stress under constant-water content condition, and (2) after wetting-induced collapse. Results show that changes in void ratio are less significant during constant-water compression (stage 0 to 1) than those corresponding to collapse upon wetting (stage 1 to 2). The compression index of unsaturated specimens increases due to saturation (stage 1 to 2), resulting in more compressibility upon wetting (Alonso et al. 1990). In contrast to constant water compression, saturation (stage 1 to 2) destroys the air-water menisci resulting in a significant reduction in void ratio.

Fig. 5(b) summarizes the results of collapse tests on recompacted and intact loess from stage zero to two. Results are presented in terms of changes in void ratio as well as volumetric strain. If it is assumed that measured data in Fig. 5(b) follow a parabolic trend, the maximum collapse occurred at vertical effective stress of nearly 150 and 200 kPa for recompacted and intact loess, respectively. A possible explanation is that the natural specimens were subjected to many cycles of drying and wetting in the field, resulting in much larger yield stress. According to the elastoplastic models for unsaturated soils (e.g., Alonso et al. 1990), wetting induced smaller plastic contraction when the initial yield stress is larger. Therefore, a higher stress level is required for occurrence of the maximum collapse potential for intact loess compared to recompacted one.

Comparison of results with those on similar soils clarifies that measured volumetric collapse strain is larger than previously reported values for intact loess. The maximum collapse stress could be greater than or equal to 200 kPa in this study. Maximum collapse potential of 3.8% was reported by Munoz-Castelblanco et al. (2011) for an undisturbed natural loess with a significantly lower *in-situ* void ratio of 0.85 than that of this study. Since the collapse potential is a function of initial void ratio, a lower initial void ratio can lead to lower collapsibility (or higher stiffness). According to Munoz-Castelblanco et al. (2011), possible true cohesion caused

by carbonate bonding resulted in low *in-situ* void ratio and hence lower collapsibility at a given load as compared to the results from this study. Volumetric collapse strains of 8% and 14% upon wetting were measured by Haeri et al. (2014) for an intact loess with an average initial void ratio of 0.77 subjected to the net mean stress levels of 50 kPa and 250 kPa, respectively. These values of net mean stress are equivalent to net vertical stress values of 75 kPa and 375 kPa assuming a K_0 value of 0.5. A comparison of the results from this study and the two mentioned above reveals that the intact loess investigated in this study gave the largest volumetric strain upon wetting among the three studies. Possible reasons are (1) a higher void ratio (Table 2) and (2) lack of "true cohesion" from a cementation agent.

Figs 6(a) and (b) illustrate variations in void ratio for unsaturated tests carried out on recompacted and intact specimens, respectively. After initial state (stage zero), specimens were brought to equalisation at different suctions (stage 0 to 1). Both recompacted and intact specimens were eventually subjected to two net stress levels of 50 kPa and 200 kPa (stage 1 to 2). From stage 0 to 1, there was a small reduction in void ratio; this was because of lower shrinkage potential of specimens resulting from an initial low water content compared to that of saturated specimens (Peng and Horn 2007). It can also be seen that reduction in void ratio due to suction equalisation and constant-suction compression is significantly lower than that observed in collapse tests upon soaking. The low compressibility of unsaturated specimens was attributed to desiccation-induced high suction resulting in high stiffness of the specimens. This postulation will be also experimentally supported by a constant-water oedometer test on an air-dried specimen in the next section.

Fig. 6(c) shows the volume changes with suction because of suction equalisation (stage 0 to 1). Most of the test data fall into a narrow range of changes in void ratio from 0.02 to 0.04. Moreover, volume changes seem to be independent of suction for suction values between 8 MPa and 230 MPa. In terms of volumetric strain, suction-induced shrinkage on average (i.e. 1.48%) was almost one order of magnitude less than the maximum measured wetting-induced collapse

(Fig. 5(b)). A possible reason for negligible volume changes is the low initial dry density of test specimens. Gatabin et al. (2016) observed a significant influence of as-compacted dry density on the evolution of the void ratio with suction. The linear slope of the void ratio-suction curve ($\Delta e/\Delta \ln(s)$) reduced from 0.240 to 0.039 as dry density decreased from 1.999 to 1.672. Another important factor controlling shrinkage is the initial amount of water or the moisture ratio, $e_w = w.G_s$. The moisture ratio of test specimens at their initial state was 0.32 which was far from the saturated moisture ratio of 0.93. Based on the conceptual division of a shrinkage curve into four zones (Peng and Horn 2007), the initial moisture ratio of loess specimens seems to belong to the residual shrinkage zone or zero shrinkage zone. As a result, loess can be expected to shrink minimally under intense drying because its dry density is low and its moisture content is also low (on the dry side of optimum).

Constant-suction compression behaviour

Fig. 7(a) shows results of compression tests on unsaturated recompacted specimens. Tests were continued until the net stress of 200 kPa was reached, which is the maximum net stress considered for shear tests. In addition, an oedometer compression test was carried out on an air-dried recompacted specimen (UR-60). The environmental conditions, i.e. *RH* and temperature, experienced by the oedometer cell were monitored, giving a suction potential as high as 60 MPa on average throughout the test. According to the results of UR-60, yielding occurs at a net stress of 490 kPa. It is noted that the yield stress is defined here corresponding to the stress level delimiting the boundary between pseudo-elastic and elasto-plastic domains (Cui and Delage 1996). The yield stress is determined by intersecting two lines fitted to the linear parts of these two domains in the plane of void ratio versus net stress in arithmetic and logarithmic scales, respectively (Munoz-Castelblanco et al. 2011). Results of constant-suction compression test on intact loess are presented in Fig. 7(b). In accordance with the results of Fig. 7(a), intact specimens do not also experience elasto-plastic strains up to the net stress level of 200 kPa.

These observations, in fact, confirm the significant extension of pseudo-elastic domain as specimens dried from *in-situ* state to high suctions (Alonso et al. 1990).

The slope of compression curves in the e - ln σ_v space, κ, is nearly the same for all suctions considered for the two types of specimens. Note that κ is used to represent the swelling modulus although it was originally defined in the e - ln p' space in the Original Cam-Clay (Roscoe and Schofield 1963). It is evident that the swelling modulus, κ, is independent of the high suctions considered for both recompacted and intact loess. This is consistent with compression test results reported by Munoz-Castelblanco et al. (2011) and Jotisankasa et al. (2007), who also revealed that κ is independent of suction for both natural and artificial collapsible soils, respectively.

Shear strength

Results of six saturated tests on both recompacted and intact loess are shown in Fig. 8. Both recompacted and intact loess suggest a hardening behaviour with almost the same ultimate strength at each effective stress level. Natural loess has an effective internal friction angle of 27.7^0 and a null true cohesion as both intact and recompacted loess specimens reached almost the same ultimate strength. The measured zero "true cohesion" for intact loess was further validated by conducting a slaking test through soaking an intact specimen in distilled water following Geoguide 3 (Guide 1998). After 5 minutes of soaking, the intact specimen collapsed suggesting that the cohesion observed in the specimens is only apparent cohesion due to suction and there is no "true cohesion" in intact specimens.

Figs 9(a) and (b) plot shear stress and axial strain versus horizontal displacement, respectively, from shear tests on unsaturated recompacted loess under 50 kPa vertical stress. Corresponding results of tests under similar conditions but on intact specimens are presented in Figs 9(c) and

(d). In contrast to the results of saturated tests, results of unsaturated tests show a sharp rise to a peak strength followed by a gradual decrease until a nearly constant ultimate state was attained. A lower stiffness can be observed for the range of horizontal displacement less than 1 mm compared to the stress-strain curve immediately before the peak strength. Since there is augmentation of strength in the initial shearing stage but at a lower rate, this bi-linear stress-strain behaviour may be attributed to the partial gap between the specimens and shear box, created during the initial suction equalisation stage. A higher rate of dilation and hence strength for unsaturated recompacted loess was observed compared to the intact one. The fact that no "true cohesion" was measured for intact loess suggests that the observed differences in shear behaviour are mainly attributed to the different arrangements of soil particles in recompacted and intact loess as no significant presence of chemical bonding was captured. In other words, the conclusions made based on the findings of current study may not be comprehensive enough for natural material with some chemical bonding and hence a more complex interpretation would be required for such cases. Results of Figs 9(b) and (d) show that the critical state may have been not reached in some cases since axial strain or dilation were still developing towards the end of the tests. This observation reveals that suction can contribute to shear strength even along the residual state. In addition, a higher dilation rate can be seen for suction of 230 MPa than for suction of 8 MPa, suggesting the influence of suction in enhancing dilation.

Fig. 10 shows results of shear tests carried out under 200 kPa vertical stress. As in low stress conditions, the shear strength of unsaturated specimens rose quickly to its peak before dropping slightly with displacement in most cases. The influence of suction on dilation enhancement can be seen in Fig. 10(b) during shearing. In addition, dilation was less significant for intact loess than for the recompacted one (Figs 10(b) and (d)). The enhancement of dilatancy is caused by a modification of the soil structure. More discussion is given later, with the support of MIP test results.

Several advanced frameworks have been proposed for interpreting shear and volumetric behaviour of unsaturated soils (e.g. Toll and Ong, 2003; Alonso et al. 2010; Zhou et al. 2016; Lloret-Cabot et al. 2016). Soil water retention curve has been also embedded into these frameworks to take into account the influence of saturation state in addition to suction effects on mechanical behaviour (Gallipoli et al. 2003). Following on Alonso et al. (2010), the peak shear strength of intact and recompacted loess specimens are interpreted by using the microstructural-based framework. The expression of shear strength can be given as follows:

$$\tau = c' + \left[\left(\sigma_v - u_a\right) + S_r^e \cdot s\right]\tan\phi' \tag{2}$$

where τ is shear strength, c' is saturated effective cohesion, ϕ' is saturated effective friction angle, σ_v-u_a is the net vertical stress, S_r^e is the effective degree of saturation, and s is suction. The proposed definition of effective degree of saturation for fine-grained soils is chosen and used as follows:

$$S_r^e = \left(S_r\right)^{\alpha} \tag{3}$$

where S_r is degree of saturation and α is a material parameter, which can be calibrated by experimental data using Eq. (2). Comparison is made between experimental measurements of peak shear strength and model predictions in Figs 11(a) and (b) for recompacted and intact loess, respectively. It can be seen that the peak shear strength for both intact and recompacted specimens shows an overall increasing trend with suction but at a reduced rate. Although model predicts an increase in peak shear strength with suction initially, there is a graduate reduction towards the same saturated shear strength asymptotically at the maximum theoretical suction of 1000 MPa. The discrepancy may be attributed to the fact that effective degree of saturation approaches zero at high suctions, which in turn eliminates the contribution of suction to shear strength according to Eq. (2). As suggested by results of Fig. 11, there is no sign of decline in shear strength even towards the maximum suction. In fact, desiccation-induced high suctions has

an undeniable role in enhancement of shear strength even in the residual zone of water retention curve.

Suction and microstructural effects on shear behaviour and dilatancy

Results of vertical displacement against horizontal displacement are used to calculate the dilatancy as $-\delta V/\delta H$, where the numerator and the denominator are the increments of vertical displacement and horizontal displacement, respectively (Taylor 1948). Data points are selected in such a way that a smooth curve can be obtained. Note that a positive sign of dilatancy means dilation of soil specimens due to shearing. Fig. 12 illustrates variations in dilatancy with horizontal displacement for all unsaturated tests. Results show that unsaturated recompacted and intact loess dilated during the whole shearing stage except at the very beginning of the tests (< 1 mm). Following the initial contraction, there was a steep rise in dilatancy up to a peak and gradual reduction afterwards. Although dilation was still in progress at the end of the shearing stage for tests conducted under 50 kPa (Figs 12(a) and (c)), it vanished in the case of specimens compressed to 200 kPa net stress (Figs 12(b) and (d)). Comparisons of unsaturated tests results in each sub-figure reveal the influence of suction on enhancing dilatancy. Since it is not easy to compare between results for the whole shearing stage as well as different net stresses and microstructures, the maximum dilatancy is measured for each unsaturated test for the sake of comparison.

Figs 13(a) and (b) show variations in the maximum dilatancy with suction for the loess specimens under 50 kPa and 200 kPa net stress levels, respectively. According to the figure, dilatancy increased linearly with suction for both types of specimens tested. Measured data for four series of unsaturated tests in Fig. (13) were analysed to quantify the influence of suction on dilation angle. Results of regression analysis reveal that for the suction range studied between 8 MPa to 230 MPa, there is an average 6.2° increase in dilation angle, suggesting 22% suction-induced increase in saturated friction angle of 27.7^0. Dilation occurred at high suction in the

order of hundreds of MPa may be different from that commonly referred to in classical soil mechanics context. The reason is that dilation is commonly attributed to the rotation and rearrangement of individual particles while for highly desiccated fine-grained soils, dilation is very likely due to the relative displacement of broken blocks. Indeed, further research is required to reveal the fundamental mechanism behind this phenomenon.

In order to eliminate effects of density on observed trends, relative compaction (*RC*) is selected as a relevant state index for loess. Numbers close to the symbols are *RC* values for soil specimens before shearing (Table 3). Results show that standard deviation and the coefficient of variation in *RC* values are 1.9% and 2.4% for intact specimens, respectively. Considering the unavoidable natural variability in density of intact specimens, these initial state indices may be considered very similar for the purpose of comparison. Results therefore reveal the significant role of suction in enhancing dilation almost as an independent parameter. A possible explanation is the suction-induced stiffening (Hoyos et al. 2014) and hence aggregation of larger clay-silt assemblies. Merchán et al. (2011) also observed a consistent increase in residual friction angle of clay with suction, and attributed it to the prevailing aggregated structure at elevated suction. Chávez and Alonso (2003) attributed the enhanced dilatancy of a compacted gravel of shale at low *RH* values to generation of stronger particles favouring dilation. According to Fig. 13(a), recompacted loess showed consistently and considerably higher dilation angles than intact loess in contrast to the observations of Zhan and Ng (2006) for an unsaturated expensive clay. The higher dilatancy of intact clay specimens was attributed to the cementation of iron and manganese oxides. The difference in maximum dilation angle of recompacted and intact loess was 9^0 on average (Fig. 13(a)). The considerable difference in the dilatancy and hence shear behaviour of soil specimens of the same type and with similar void ratios reflects the microstructural effects which will be discussed in the next section.

Fig. 13(b) shows variations in the maximum dilatancy/dilation angle with suction for specimens compressed to 200 kPa net stress. Dilatancy increased linearly with suction for both

recompacted and intact loess although the void ratio of recompacted specimens varied by less than 0.01 after compression. This observation highlights the substantial influence of suction on the dilation angle of recompacted loess. However, the void ratio of intact specimens tested under 200 kPa varied much more and by 0.13 in one case, which could be a consequence of natural variability. Nevertheless, suction effects on the dilatancy of intact specimens under 200 kPa net stress cannot be neglected. The higher dilatancy of recompacted loess is attributed to its different microstructure from that of intact loess. In addition, comparison between Figs 13(a) and (b) reveals considerable influence of net stress on reducing the dilation angle independent of the type of material tested (i.e. recompacted or intact). The increase in net stress masked the suction effects and hence suppressed the dilation due to shearing.

MICROSTRUCTURE AND SHEAR BEHAVIOUR

Interpretation of MIP test results

A total of six MIP tests on freeze-dried specimens were conducted to explore the microstructure of loess at different suction values. Three suction levels of 0.1 MPa (corresponding to *in-situ*/as-compacted state), 8 MPa, and 230 MPa were chosen and the test conditions are summarised in Table 4. Fig. 14(a) illustrates pore size density (PSD) functions of recompacted specimens. The three curves are quantitatively similar although the MR-8 and MR-230 specimens were subjected to severe drying processes. Results indicate a clear peak near 11 μm corresponding to the dominant size of macropores (d_M). However, the peak corresponding to the dominant size of micropores (d_m) in the range of 0.04 and 0.1 μm was much less pronounced. The delimiting diameter of microporosity and macroporosity was derived from the PSD functions, where the derivative with respect to the abscissa becomes zero.

Fig. 14(b) shows MIP test results in terms of the cumulative void ratio as a function of entrance diameter. The maximum values represent the MIP void ratio, e_{MIP}. Consistent with the macroscopic measurements (Fig. 6(b)), the as-compacted specimen delivered a higher e_{MIP} than

the other two dried specimens because of the shrinkage induced by suction, but the volumetric contraction was negligible. If all pores inside the test specimens can be intruded by mercury and hence detected by the MIP apparatus, e_{MIP} should be equal to e. But MIP cannot detect pores smaller than a certain diameter as well as pores larger than a certain diameter, being dictated by the maximum and minimum mercury pressure, respectively. Results reported by Ng et al. (2016) confirmed that all existing pores inside the intact loess were larger than the minimum detectable diameter of 5 nm. Therefore, MIP test results can be used to reliably evaluate the microporosity of loess. PSD functions of intact loess are plotted in Fig. 14(c). Similar to results of recompacted loess, suction changes from the *in-situ* value to severe drying would not affect the dominant sizes of micropores as well as macropores. Fig. 14(d) plots the cumulative void ratio as a function of pore diameter. By comparing Figs 14(b) and (d), it can be inferred that a smaller amount of voids can be detected for intact loess than for the recompacted one. Therefore, intact loess contains a higher proportion of non-detected voids, e_{nd} (Table 4), as a result of the existence of extra-large pores in its natural form (Ng et al. 2016; Haeri et al. 2016).

The microvoid ratio, e_m was determined based on cumulative void ratio in conjunction with the delimiting diameter. Because of a significant volume of non-detected voids (e_{nd}), information on void ratio is needed to calculate the macrovoid ratio, e_M (Alonso et al. 2013). Following this methodology, corresponding values of e_m and e_M were determined and given in Table 4. Results obtained from soil water retention data is also consistent with MIP measurements in terms of trends but not the exact magnitude. Both methodologies revealed that recompacted loess contains larger portion of e_m compared to intact one (Table 1). One possible explanation for the difference between two approaches could be the derivation of S_r^m from water retention data in a region where limited data were obtained by axis translation and vapour equilibrium techniques. A complementary approach such as osmotic method of controlling suction is hence required to fill in the gap. On the other hand, the MIP equipment well covers the corresponding range for

precise evaluation of delimiting pore size and hence MIP test results are employed to interpret the shearing behaviour.

Significance of macrovoid ratio

The microvoid ratio as well as the macrovoid ratio inferred from MIP test results are used for explaining differences in the dilatancy and hence shear behaviour of recompacted and intact loess. Fig.15 shows the distribution of void ratios (i.e. e_m and e_M) for recompacted and intact loess specimens. Comparisons are made for three different suction values. Results clearly indicate that the distribution of void ratios is not subjected to changes in suction for the range and path considered in this study. More important, differences between microvoid ratio and macrovoid ratio are more significant in the case of intact loess than the recompacted one. Although both show a non-uniform distribution of voids, the non-uniformity is more pronounced for intact loess specimens. Similar postulation was also made by Haeri et al. (2016) after comparing SEM photos of undisturbed and recompacted loess. Results of Fig. 15 confirm that the intact loess contains higher proportion of macrovoids than recompacted loess because of its smaller microporosity and larger population of large pores (Table 4). In addition, variations in the macrovoid ratio with suction confirm the independence of e_M from suction.

Fig. 16 shows the influence of macrovoid ratio on peak dilatancy of unsaturated loess at different suctions and net stress levels. According to Fig. 16(a), the maximum dilatancy decreases as the macrovoid ratio increases under net normal stress of 50 kPa. Although the maximum dilatancy is suppressed by elevating the net stress from 50 kPa to 200 kPa (Fig. 16(b)), it still decreases with an increase in macrovoid ratio. In other words, there is a clear reduction in the maximum dilatancy with an increase in macrovoid ratio for all the tests conducted. It is evident that macrovoid ratio could be better than void ratio to describe dilatancy and hence the shear strength of unsaturated loess with a special aeolian microstructure being different from sedimentary and residual soils.

Although recompacted and intact specimens exhibited similar void ratios, the differences in dilatancy and shear behaviour were very significant at all levels of applied net stress and suction. The microstructural quantifications reveal that differences in distribution of voids between recompacted and intact loess were large even for the same target void ratio. Therefore, the void ratio may not be a suitable state parameter describing shear behaviour. In fine-grained soils, silt-clay assemblies also known as aggregates are analogous to individual soil particles in a coarse-grained geomaterial. It is the void spaces between aggregates (macrovoid ratio) that are governing shear behaviour rather than the voids within individual aggregates (microvoid ratio). According to this postulation, silt-clay aggregates in unsaturated fine-grained soils are considered as individual particles. The inter-aggregate space represents the macrovoid ratio while the intra-aggregate pores are representative of microvoid ratio. The existence of this pore population may not affect the global behaviour provided that soil aggregates interact as individual rigid bodies during shearing. However, the volume of micropores in a soil with a certain void ratio would affect the volume of the associated macropores. Microstructural measurements revealed that the macrovoid ratio of the intact loess is approximately 0.2 higher than that of the recompacted loess (Fig. 15). This notable difference in e_M can be responsible for the more dilative shear behaviour of the latter than the former at different combinations of net stress and suction. Therefore, macrovoid ratio, e_M, is a more reliable state parameter than the conventionally used void ratio, e, for describing unsaturated fine-grained soil behaviour.

SUMMARY AND CONCLUSIONS

Shear strength and dilatancy of saturated and unsaturated loess at high suctions were investigated by utilising a humidity controlled shear box chamber. In addition, the microstructure of recompacted and intact loess was quantified through MIP experiments at different suction levels. Based on these test results, the following conclusions can be drawn:

1. During shearing, saturated specimens exhibited contractive behaviour. In contrast, unsaturated specimens dilated. A continuous increase in the peak shear strength was observed with suction ranging from 8 to 230 MPa. This was probably due to the observed increase in dilatancy with suction. At a given net stress, the dilatancy of recompacted and intact loess increased linearly with suction.
2. Macroscopic and microstructural evaluations of void ratio confirmed that the observed increase in dilatancy with an increase in suction is not governed by a change in void ratio but depends on the microstructure and the distribution between micro and macroporosity. Under similar test conditions, recompacted loess consistently showed higher dilatancy than that of intact loess.
3. At a given void ratio, recompacted and intact loess showed different distributions of micropores and macropores because they had different initial microstructures resulting from sample preparation and natural occurrence in the field, respectively. Analysis of the MIP test results confirmed that the distribution of voids was more uniform in recompacted loess than that in intact loess, due to a relatively larger number of large pores present in the intact loess. It was therefore proposed that a macrovoid ratio, e_M, can be used to quantify the difference in their microstructures. The observed e_M of intact loess was about 0.2 higher than that of recompacted loess, consistent with the measured lower dilatancy of intact than that of recompacted loess at given stress and suction conditions.

ACKNOWLEDGEMENTS

The authors would like to greatly acknowledge National Natural Science Foundation of China's grant number 51778166 and the Research Grants Council of the Hong Kong Special Administrative Region (HKSAR) for providing financial support of the presented work through the research grants 16209415, 16216116 and 16212218. The second author is also very grateful

to the Office of Vice-President for Research and Technology of Sharif University of Technology for the financial support provided.

NOTATION

c' Saturated effective cohesion

D Dilatancy

d_m Dominant pore size diameter of microvoids

d_M Dominant pore size diameter of macrovoids

d_{max} Maximum dilatancy

e Void ratio

e_{ave} Average void ratio

e_m Microvoid ratio

e_M Macrovoid ratio

e_{max} Maximum void ratio

e_{min} Minimum void ratio

e_{MIP} Cumulative intrusion void ratio of MIP test

e_{nd} Non-detected void ratio

e_w Moisture ratio

G_s Specific gravity

PSD Pore size density function

RC Relative compaction

RH Relative humidity

s Suction

S_r Degree of saturation

S_r^e Effective degree of saturation

S_r^m Microstructural degree of saturation

u Horizontal displacement

u_a Pore air pressure

w Gravimetric water content

α Material parameter in Eq. (3)

δH Increment of horizontal displacement

δV Increment of vertical displacement

ε_v Volumetric strain

ε_y Vertical strain

κ Recompression index under K_0 loading conditions

λ Compression index

ξ_m Microstructural parameter

σ_v-u_a Net vertical stress

σ'_v Effective vertical stress

τ Shear stress

ϕ'_{cs} Effective critical state friction angle

ψ Angle of dilation

REFERENCES

Alonso, E.E., Gens, A., and Josa, A. 1990. A constitutive model for partially saturated soils. Géotechnique, **40**(3): 405–430.

Alonso, E.E., Iturralde, E.F.O., and Romero, E.E. 2007. Dilatancy of coarse granular aggregates. In: Schanz T. (eds) Experimental Unsaturated Soil Mechanics. Springer Proceedings in Physics, **112**. Springer, Berlin, Heidelberg.

Alonso, E.E., Pereira, J.M., Vaunat, J., and Olivella, S. 2010. A microstructurally based effective stress for unsaturated soils. Géotechnique, **60**(12): 913-925.

Alonso, E.E., Pinyol, N.M., and Gens, A. 2013. Compacted soil behaviour: Initial state, structure and constitutive modelling. Géotechnique, **63**(6): 463–478.

Alsherif, N.A., and McCartney, J.S. 2015. Thermal behaviour of unsaturated silt at high suction magnitudes. Géotechnique, **65**(9): 703-716.

ASTM. 2000. Standard test method for consolidated undrained direct simple shear testing of cohesive soils, ASTM standard D6528. American Society for Testing and Materials, West Conshohocken, Pa.

ASTM. 2011a. Standard practice for classification of soils for engineering purposes (Unified Soil Classification System). ASTM standard D2487. American Society for Testing and Materials, West Conshohocken, Pa.

ASTM. 2011b. Standard test methods for maximum index density and unit weight of soils using a vibratory table. ASTM standard D4253. American Society for Testing and Materials, West Conshohocken, Pa.

ASTM. 2011c. Standard test methods for minimum index density and unit weight of soils and calculation of relative density. ASTM standard D4254. American Society for Testing and Materials, West Conshohocken, Pa.

Been, K., and Jefferies, M.G. 1985. A state parameter for sands. Géotechnique, **35**(2): 99–112.

Blatz, J.A., Cui, Y.J., and Oldecop, L. 2008. Vapour equilibrium and osmotic technique for suction control. Geotechnical and Geological Engineering, **26**(6): 661–673.

Bolton, M.D. 1986. Strength and dilatancy of sands. Géotechnique, **36**(1): 65–78.

Chávez, C., and Alonso, E.E. 2003. A constitutive model for crushed granular aggregates which includes suction effects. Soils and Foundations, **43**(4): 215–227.

Chiu, C.F., and Ng, C.W.W. 2003. A state-dependent elasto-plastic model for saturated and unsaturated soils. Géotechnique, **53**(9): 809-830.

Cui, Y.J., and Delage, P. 1996. Yielding and plastic behaviour of an unsaturated compacted silt. Géotechnique, **46**(2): 291–311.

Delage, P., Tessier, D., and Audiguier, M.M. 1982. Use of the Cryoscan apparatus for observation of freeze-fractured planes of a sensitive Quebec clay in scanning electron microscopy. Canadian Geotechnical Journal, **19**(1): 111–114.

Gallipoli, D., Gens, A., Sharma, R., and Vaunat, J. 2003. An elasto-plastic model for unsaturated soil incorporating the effects of suction and degree of saturation on mechanical behaviour. Géotechnique, **53**(1): 123–135

Gatabin, C., Talandier, J., Collin, F., Charlier, R., and Dieudonné, A. 2016. Competing effects of volume change and water uptake on the water retention behaviour of a compacted MX-80 bentonite/sand mixture. Applied Clay Science, **121-122**: 57–62.

Gibbs, H.J., and Holland, W.Y. 1960. Petrographic and engineering properties of loess. Bureau of Reclamation, US Department of the Interior, Denver, CO.

Guide to rock and soil descriptions (GEOGUIDE). 1998. Geotechnical Control Office, Public Works Department of Hong Kong, Hong Kong.

Haeri, S.M., Garakani, A.A., Khosravi, A., and Meehan, C.L. (2014). Assessing the hydro-mechanical behavior of collapsible soils using a modified triaxial test device. Geotechnical Testing Journal, **37**, 2.

Haeri, S.M., Khosravi, A., Garakani, A.A., and Ghazizadeh, S. 2016. Effect of Soil Structure and Disturbance on Hydromechanical Behavior of Collapsible Loessial Soils. International Journal of Geomechanics, 04016021.

Hoyos, L.R., Velosa, C.L., and Puppala, A.J. 2014. Residual shear strength of unsaturated soils via suction-controlled ring shear testing. Engineering Geology, **172**: 1–11.

Jotisankasa, A., Ridley, A., and Coop, M. 2007. Collapse behavior of compacted silty clay in suction-monitored oedometer apparatus. Journal of Geotechnical and Geoenvironmental Engineering, **133**(7): 867–877.

Lloret-Cabot, M., Wheeler, S.J., and Sánchez, M. 2016. A unified mechanical and retention model for saturated and unsaturated soil behaviour. Acta Geotechnica, 1-21.

Li, P., Zhao, Y., and Zhou, X. 2016. Displacement characteristics of high-speed railway tunnel construction in loess ground by using multi-step excavation method. Tunnelling and Underground Space Technology, **51**: 41-55.

Merchán, V., Romero, E., and Vaunat, J. 2011. An adapted ring shear apparatus for testing partly saturated soils in the high suction range. Geotechnical Testing Journal, **34**, 5.

Munoz-Castelblanco, J.A., Pereira, J.M., Delage, P., and Cui, Y.J. 2012. The water retention properties of a natural unsaturated loess from northern France. Géotechnique, **62**(2): 95–106.

Munoz-Castelblanco, J., Delage, P., Pereira, J.M., and Cui, Y.J. 2011. Some aspects of the compression and collapse behaviour of an unsaturated natural loess. Géotechnique letter, **1**(2): 17–22.

Ng, C.W.W., Baghbanrezvan, S., Sadeghi, H., Zhou, C., and Jafarzadeh, F. 2017a. Effect of specimen preparation techniques on dynamic properties of unsaturated fine-grained soil at high suctions. Canadian Geotechnical Journal, **54**(9): 1310-1319.

Ng, C.W.W., and Chiu, A.C.F. 2003. Laboratory study of loose saturated and unsaturated decomposed granitic soil. Journal of Geotechnical and Geoenvironmental Engineering, **129**(6): 550–559.

Ng, C.W.W., Sadeghi, H., Hossen, S.B., Chiu, C., Alonso, E.E., and Baghbanrezvan, S. 2016. Water retention and volumetric characteristics of intact and re-compacted loess. Canadian Geotechnical Journal, **53**(8): 1258–1269.

Ng, C.W.W., Sadeghi, H., and Jafarzadeh, F. 2017b. Compression and shear strength characteristics of compacted loess at high suctions. Canadian Geotechnical Journal, **54**(5): 690–699.

Ng, C.W.W., Wong, H.N., Tse, Y.M., Pappin, J.W., Sun, H.W., Millis, S.W., and Leung, A.K. 2011. A field study of stress-dependent soil–water characteristic curves and permeability of a saprolitic slope in Hong Kong. Géotechnique, **61**(6): 511–521.

Ng, C.W.W., and Zhou, R.Z.B. 2005. Effects of soil suction on dilatancy of an unsaturated soil. Proceedings of the 16th International Conference on Soil Mechanics and Geotechnical Engineering: Geotechnology in Harmony with the Global Environment **2**: 559–562.

Nishimura, T. 2016. Influence of shear speed on hydro-mechanical behavior for compacted bentonite. Japaneas Geotechnical Socicety Special Publication, **2**(53): 1837-1840.

Nishimura, T., and Vanapalli, S.K. 2005. Volume change and shear strength behavior of an unsaturated soil with high soil suction. 16th International Conference on Soil Mechanics and Geotechnical Engineering, 563-566.

Patil, U.D., Hoyos, L.R., and Puppala, A.J. 2015. Suitable shearing rate for triaxial testing of intermediate soils under vapor controlled medium to high suction range. IFCEE 2015, ASCE, 2141-2150.

Patil, U.D., Hoyos, L.R., and Puppala, A.J. 2016. Characterization of compacted silty sand via relative humidity-controlled triaxial testing. 3rd European Conference on Unsaturated Soils – "E-UNSAT 2016", 09012.

Peng, X., and Horn, R. 2007. Anisotropic shrinkage and swelling of some organic and inorganic soils. European Journal of Soil Science, **58**(1): 98–107.

Potts, D.M., Dounias, G.T., and Vaughan, P.R. 1987. Finite element analysis of the direct shear box test. Géotechnique, **37**(1): 11-23.

Roscoe, K.H., and Schofield, A.N. 1963. Mechanical behaviour of an idealised wet clay. 2nd European Conference on Soil Mechanics and Foundation Engineering (ECSMFE), Wiesbaden, **1**: 47–54.

Rowe, P.W. 1962. The stress–dilatancy relation for static equilibrium of an assembly of particles in contact. Proc. R. Soc. London Ser. A **269**: 500–527.

Sadeghi, H. 2016. A micro-structural study on hydro-mechanical behavior of loess. Dual-degree PhD thesis, Hong Kong University of Science and Technology and Sharif University of Technology.

Sadeghi, H., Chiu, C.F., Ng, C.W.W., and Jafarzadeh, F. 2018. A vacuum-refilled tensiometer for deep monitoring of *in-situ* pore water pressure. Scientia Iranica. https://doi.org/10.24200/SCI.2018.5052.1063

Sadeghi, H., Jafarzadeh, F., and Ng, C.W.W. 2017. A VET-based direct shear box for testing unsaturated soils at high suctions. PanAm-UNSAT 2017: Unsaturated Soil Mechanics for Sustain-able Geotechnics, Dalas, TX, USA, 258–267.

Sadeghi H., Kiani M., Sadeghi M., and Jafarzadeh F. 2019. Geotechnical characterization and collapsibility of a natural dispersive loess. Engineering Geology, **250**: 89–100. https://doi.org/10.1016/j.enggeo.2019.01.015

Taylor, D.W. 1948. Fundamentals of Soil Mechanics. Wiley, New York.

Toll, D.G., and Ong, B.H. 2003. Critical-state parameters for an unsaturated residual sandy clay. Géotechnique, **53**(1): 93-103.

Wen, B., and Yan, Y. 2014. Influence of structure on shear characteristics of the unsaturated loess in Lanzhou, China. Engineering Geology, **168**: 46–58.

Wheeler, S.J., and Sivakumar, V. 1995. An elasto-plastic critical state framework for unsaturated soil. Géotechnique, **45**(1): 35–53.

Zhan, T.L.T., and Ng, C.W.W. 2006. Shear strength characteristics of an unsaturated expansive clay. Canadian Geotechnical Journal, **43**(7): 751–763.

Zhou, A., Huang, R., and Sheng, D. 2016. Capillary water retention curve and shear strength of unsaturated soils. Canadian Geotechnical Journal, **53**(6): 974-987.

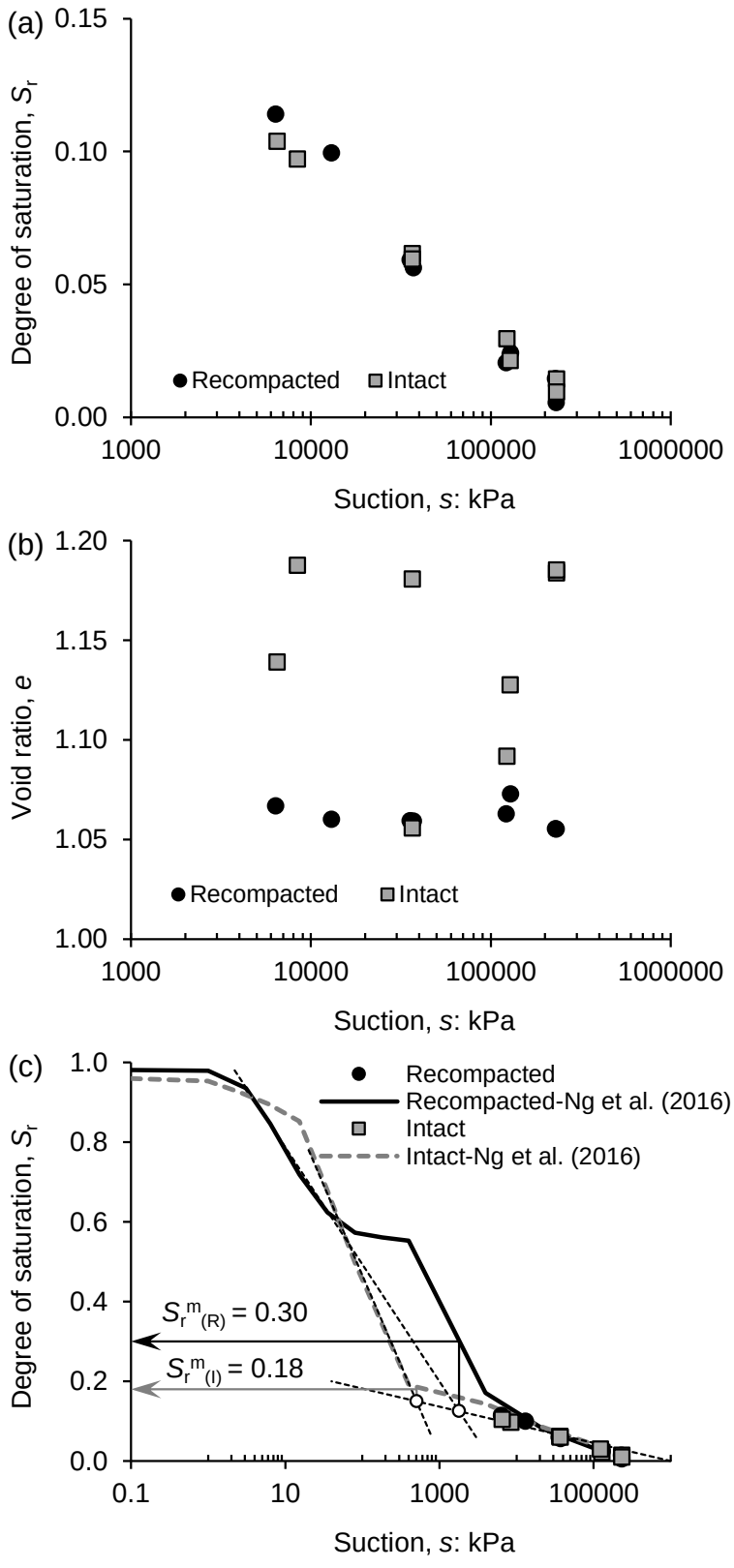

Fig. 1. Water retention and volumetric properties of studied loess

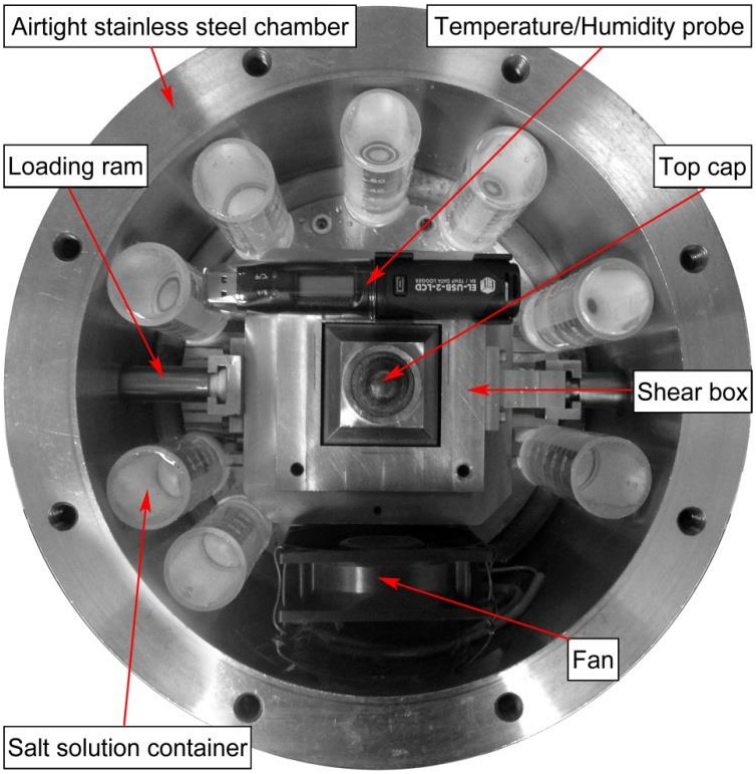

Fig. 2. Plan view of the modified direct shear box device

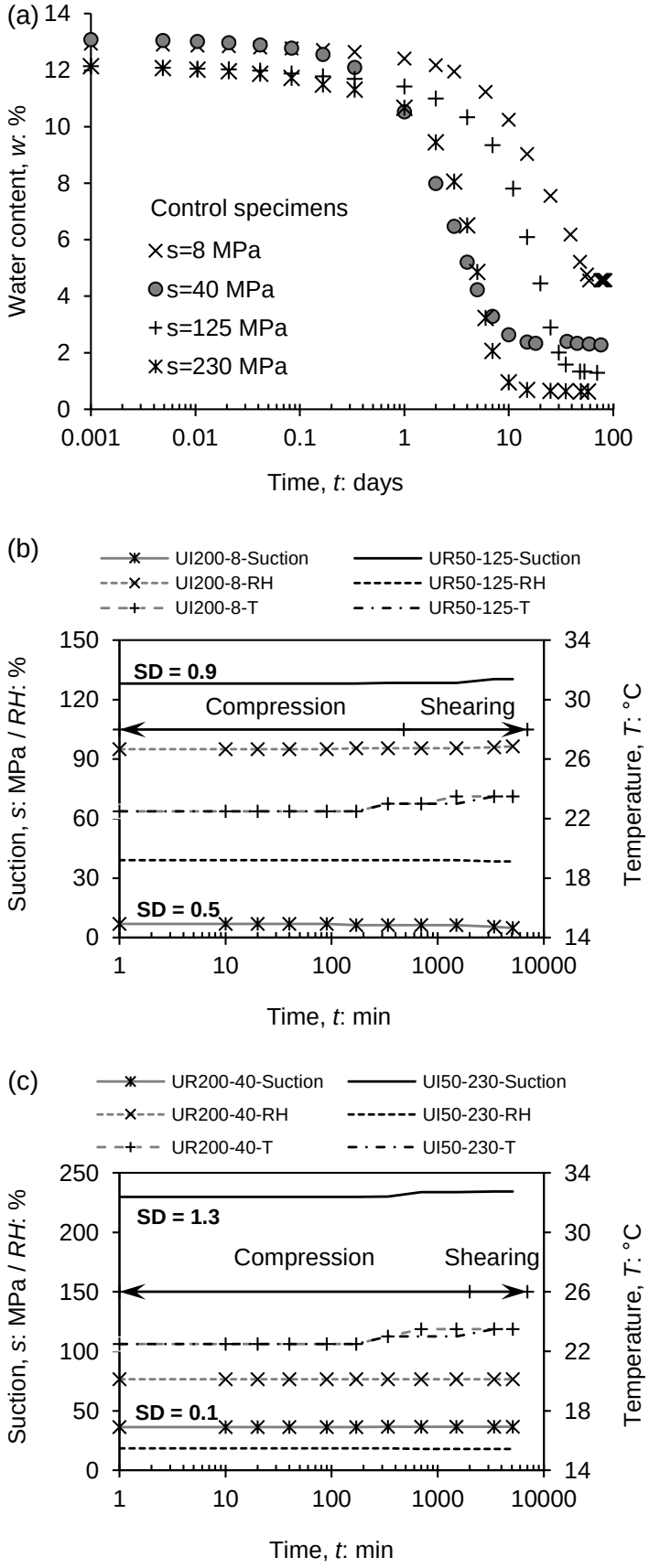

Fig. 3. (a) Typical suction equalization curves, and environmental conditions inside the shear box chamber for suction values of (b) 8 & 125 MPa, and (c) 40 & 230 MPa

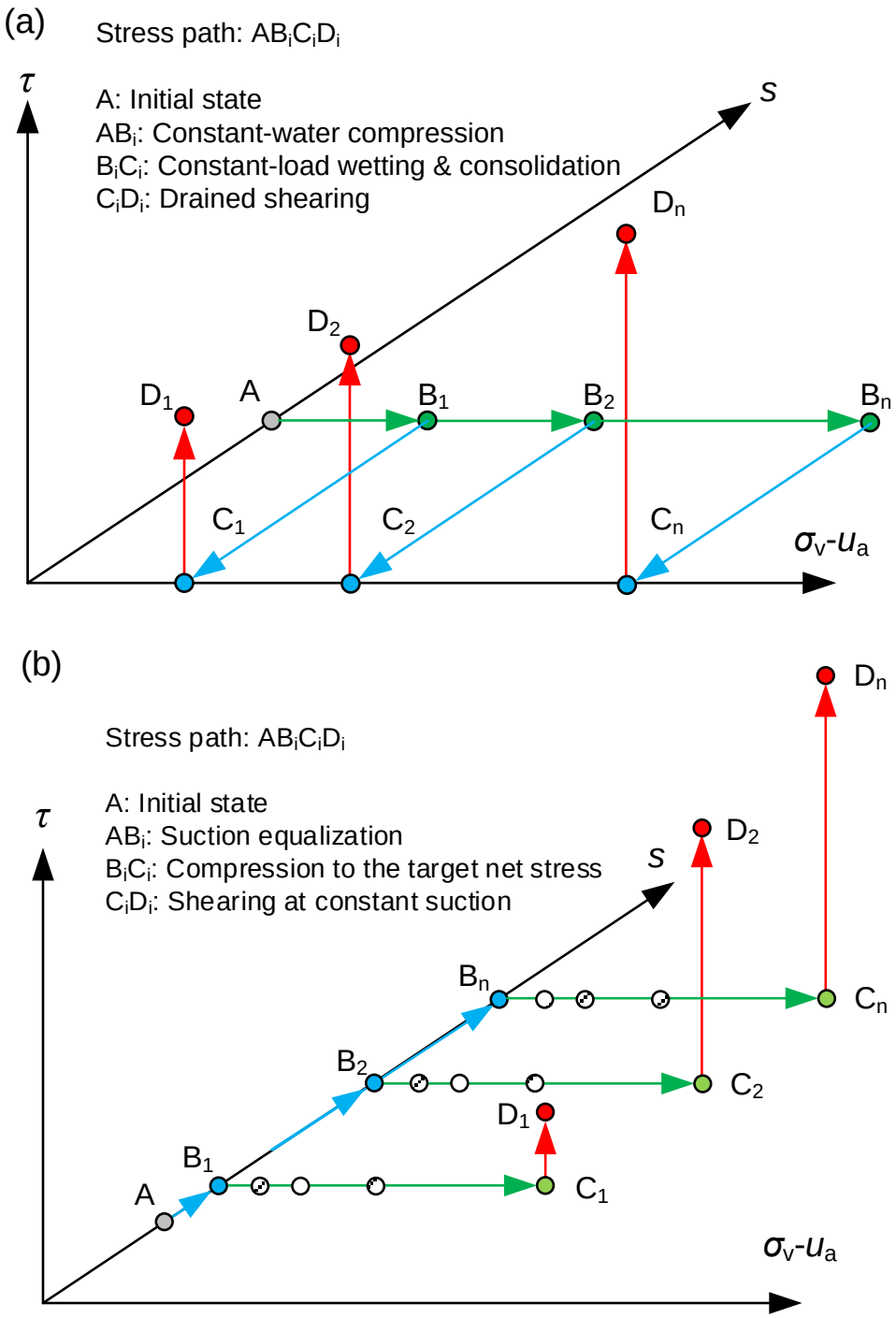

Fig. 4. Stress paths followed in (a) saturated tests and (b) unsaturated tests

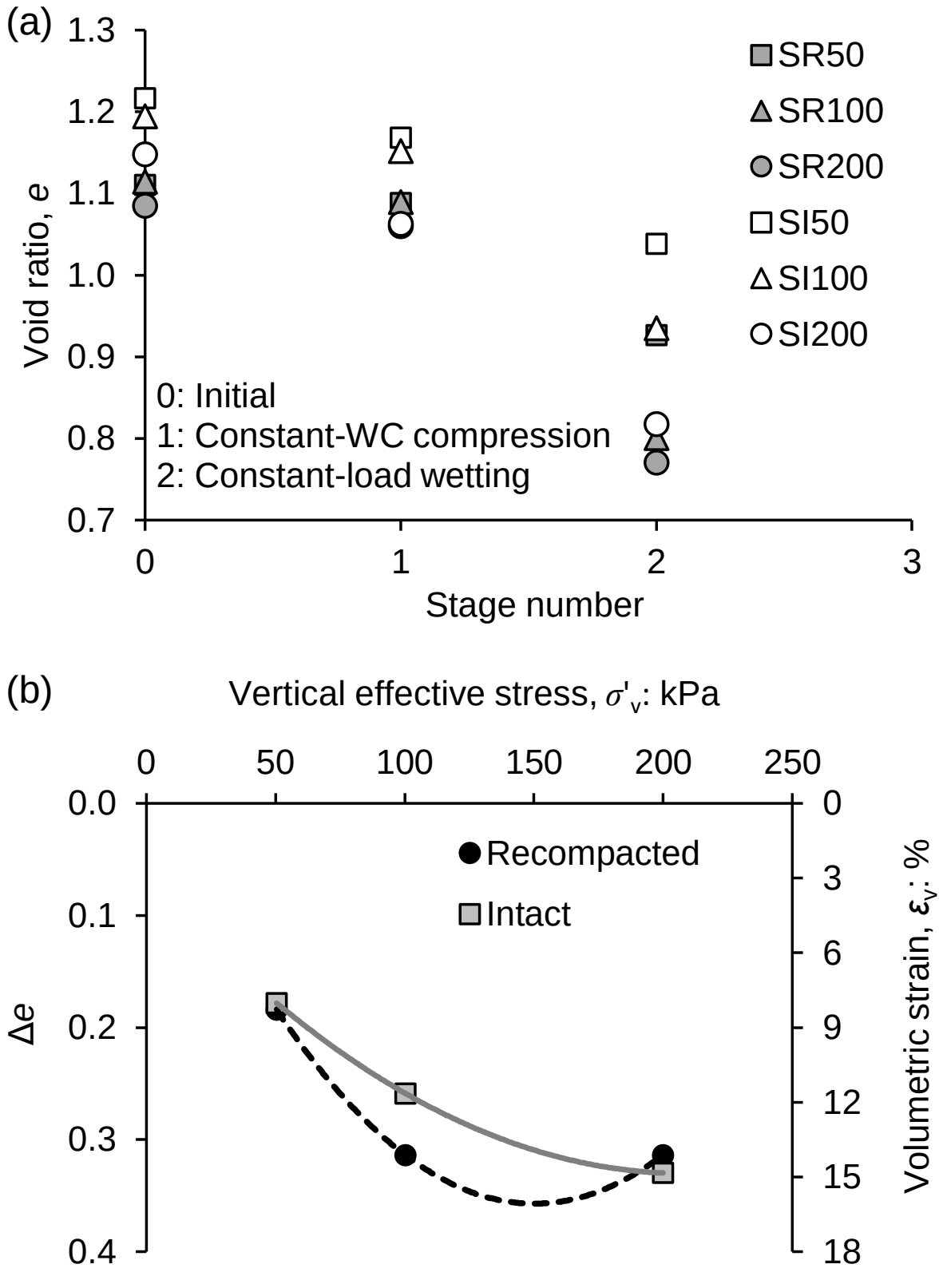

Fig. 5. (a) Variations in void ratio of saturated tests at different stages and (b) volume changes due to constant-load wetting

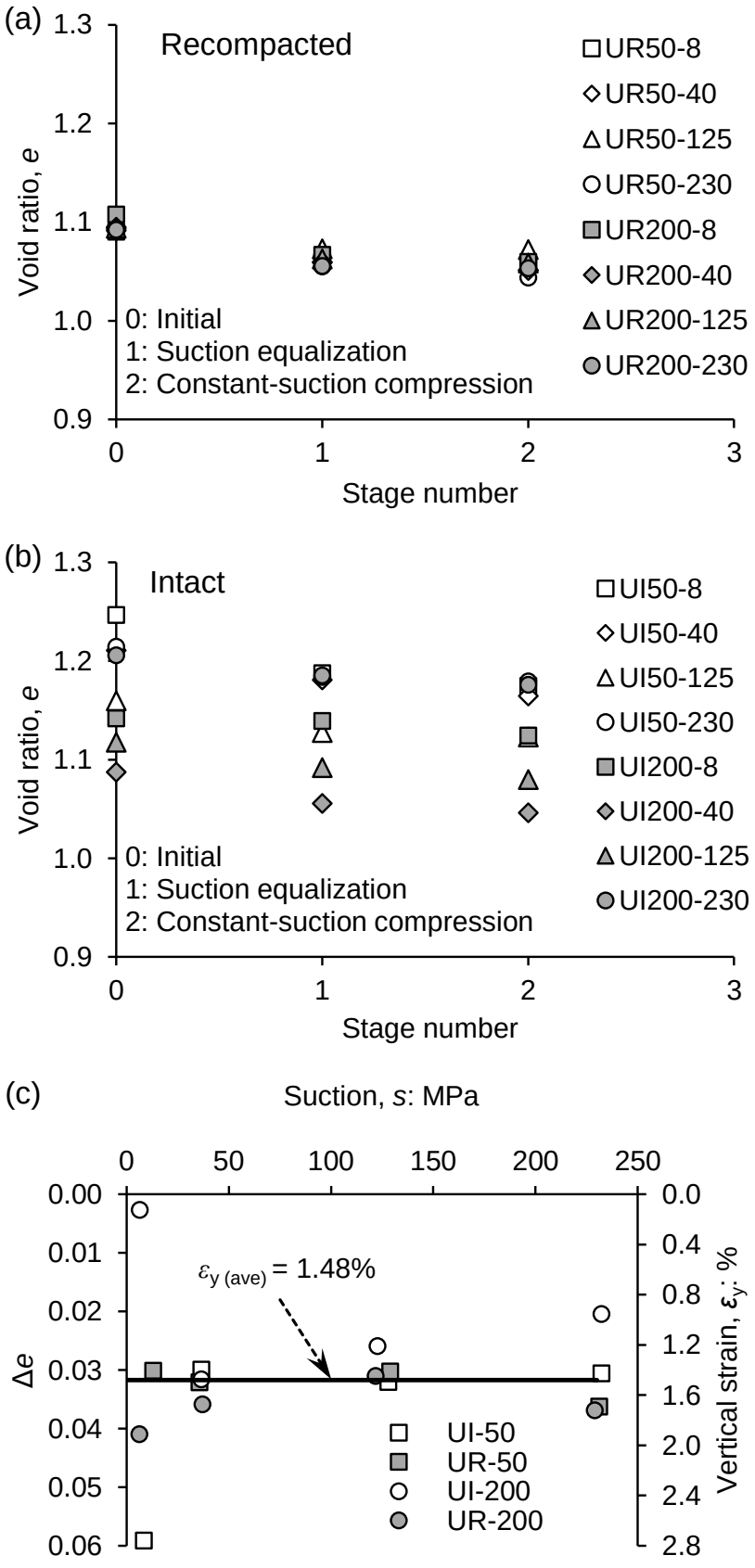

Fig. 6. Variations in void ratio of unsaturated tests at different stages for (a) recompacted and (b) intact specimens and (c) volume changes due to suction equalization

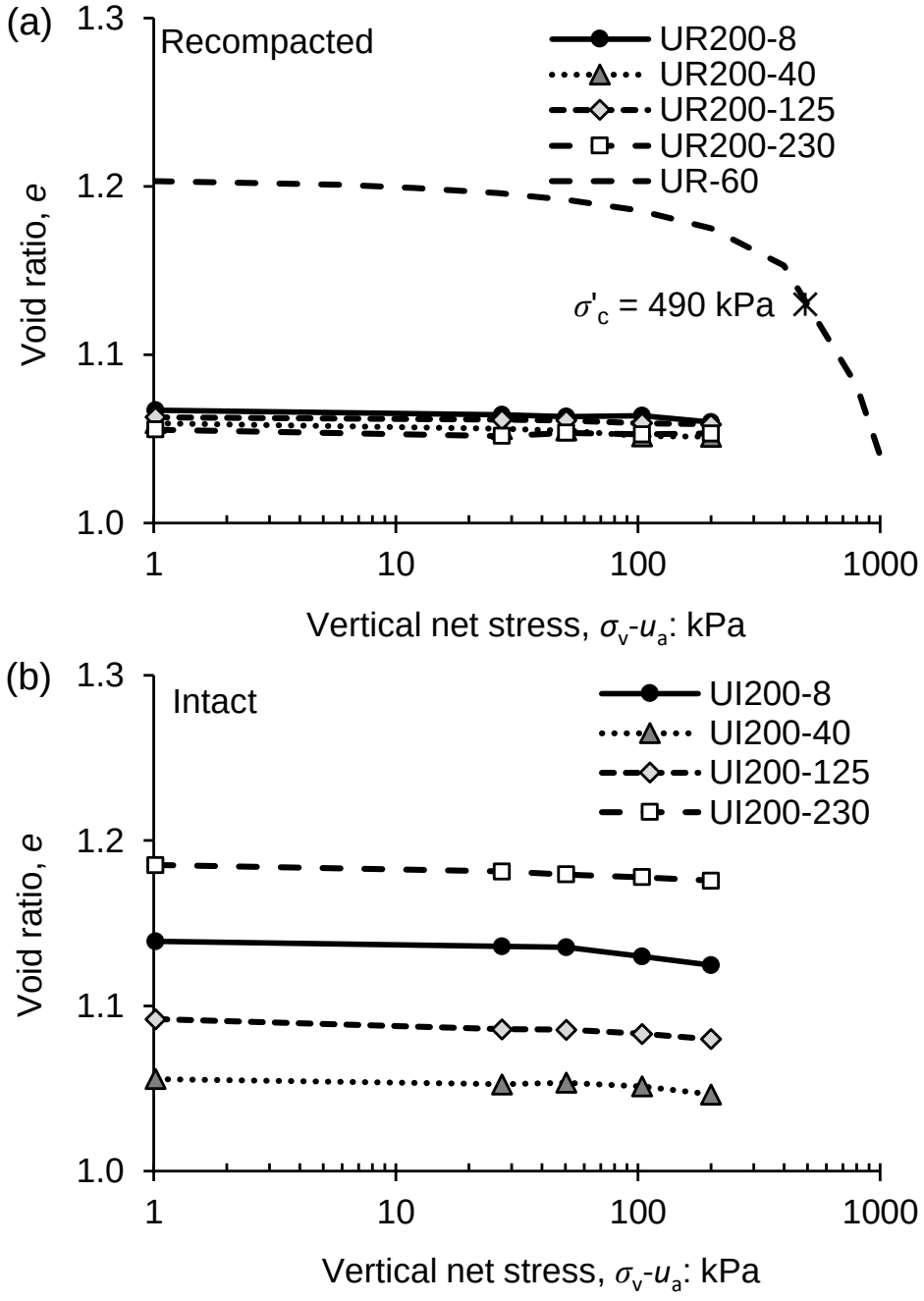

Fig. 7. Compressions of unsaturated (a) recompacted loess and (b) intact loess

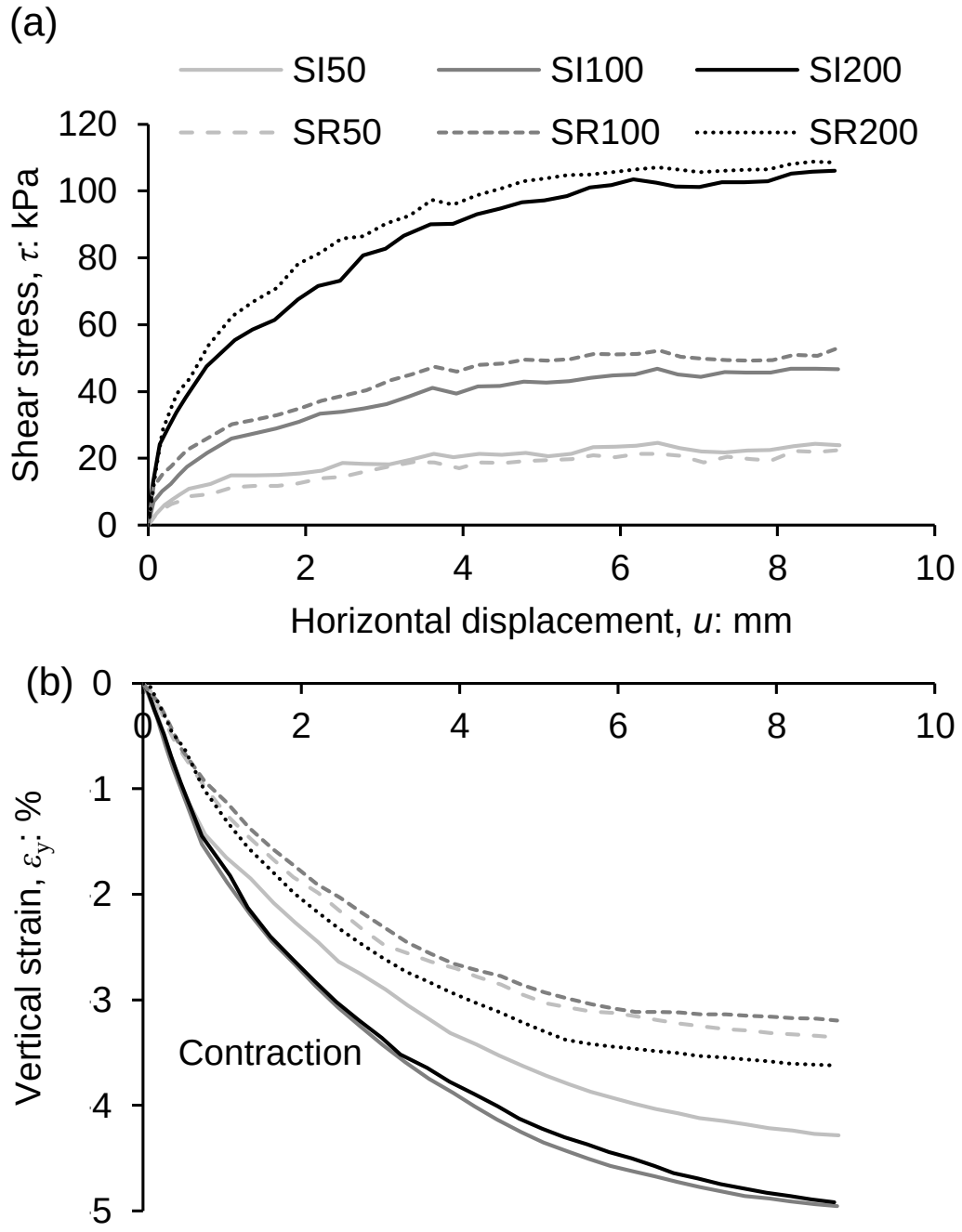

Fig. 8. Shear behaviour of saturated recompacted and intact loess; (a) shear stress, and (b) vertical strain versus horizontal displacement

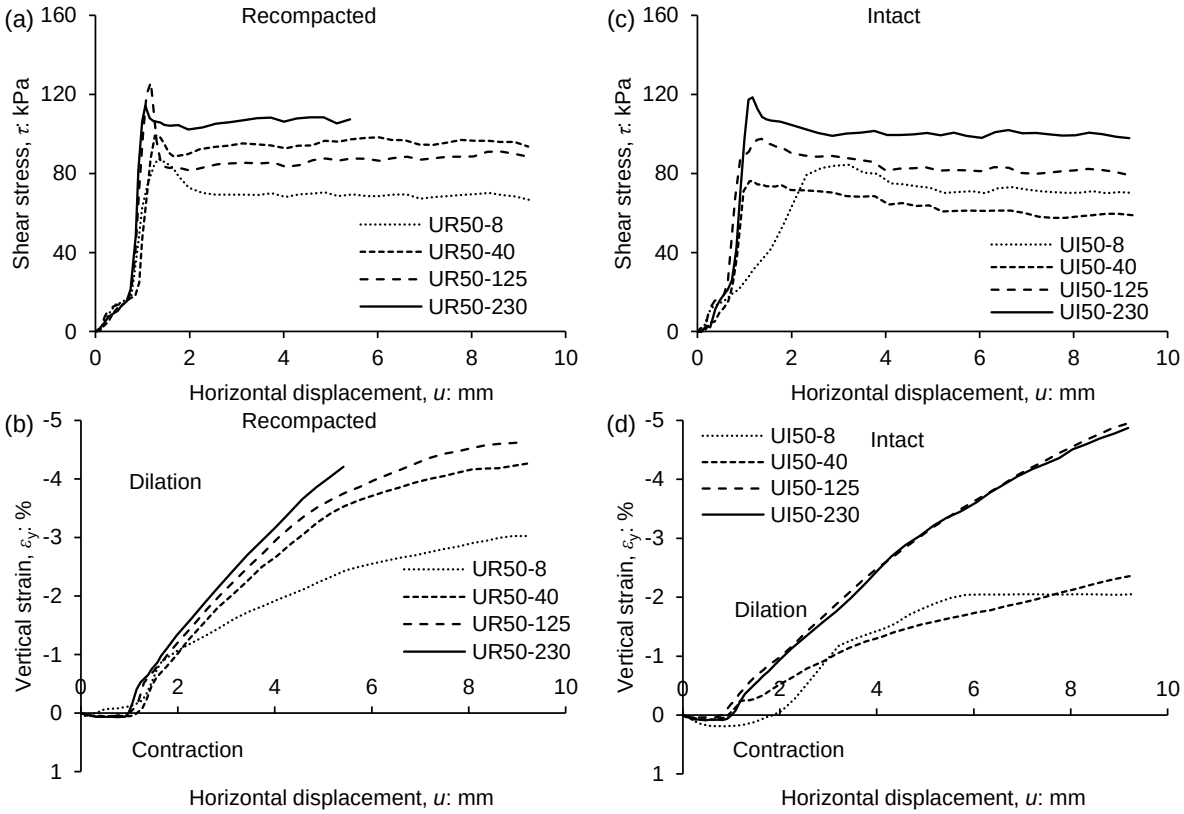

Fig. 9. Shear behaviour of (a) & (b) recompacted loess and (c) & (d) intact loess under 50 kPa of vertical stress

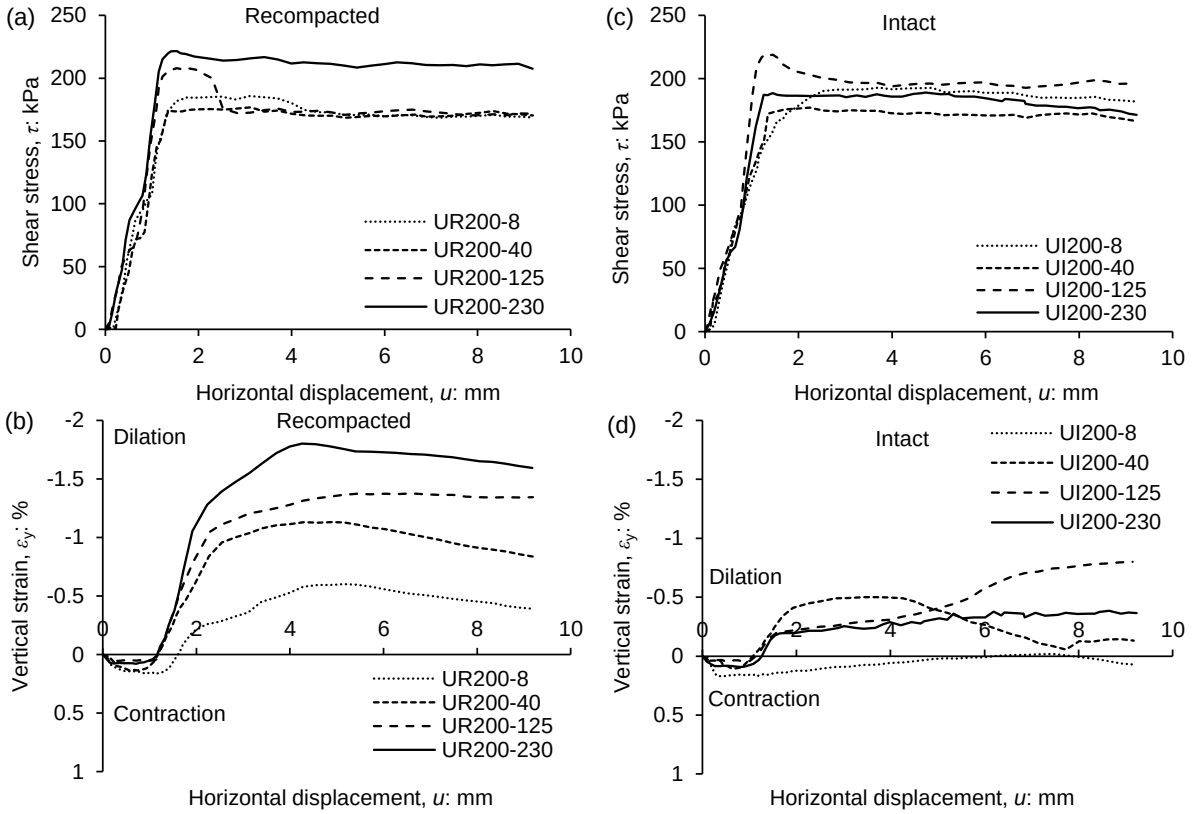

Fig. 10. Shear behaviour of (a) & (b) recompacted loess and (c) & (d) intact loess under 200 kPa of vertical stress

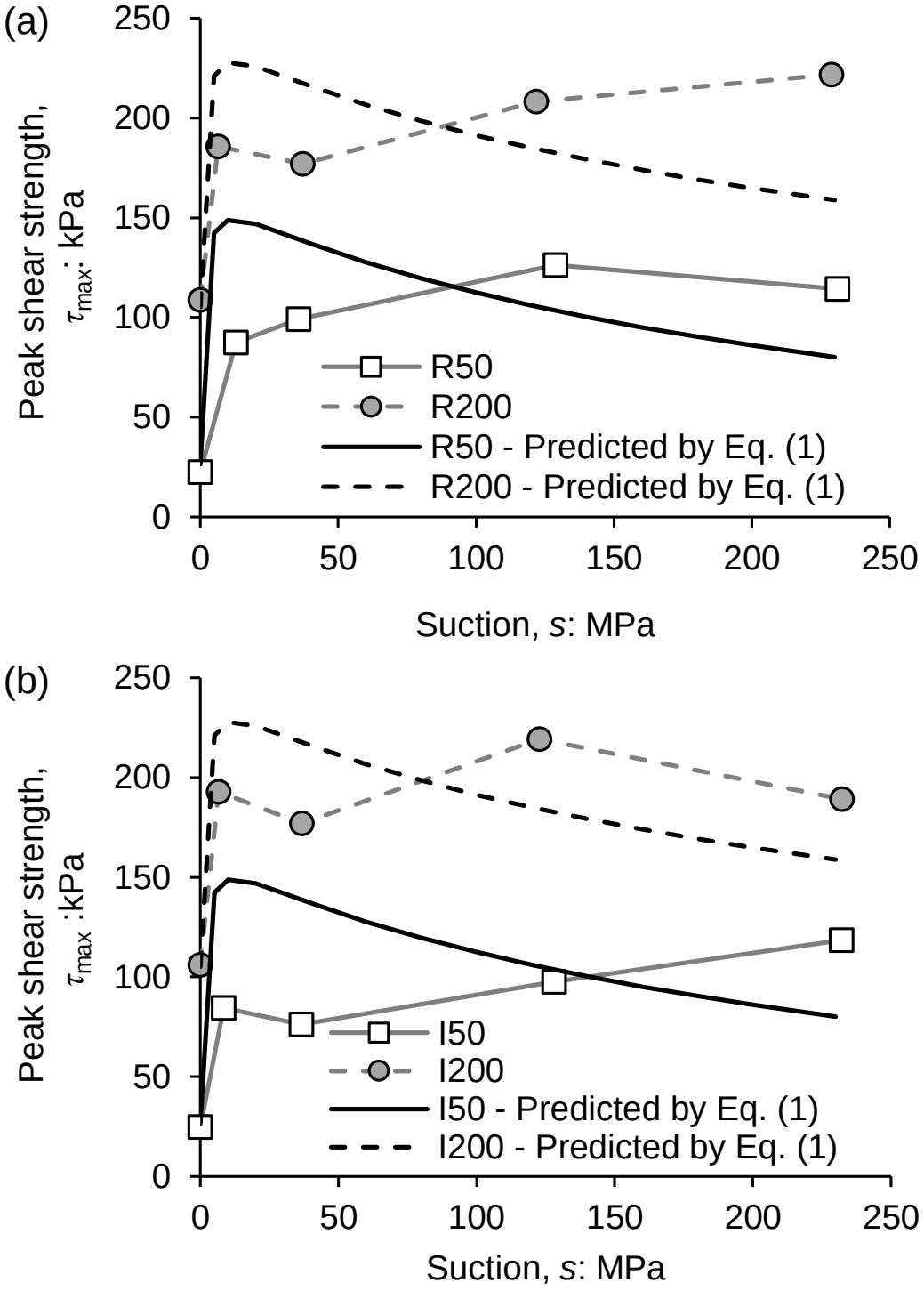

Fig. 11. Variations in peak shear strength with suction (a) recompacted and (b) intact specimens

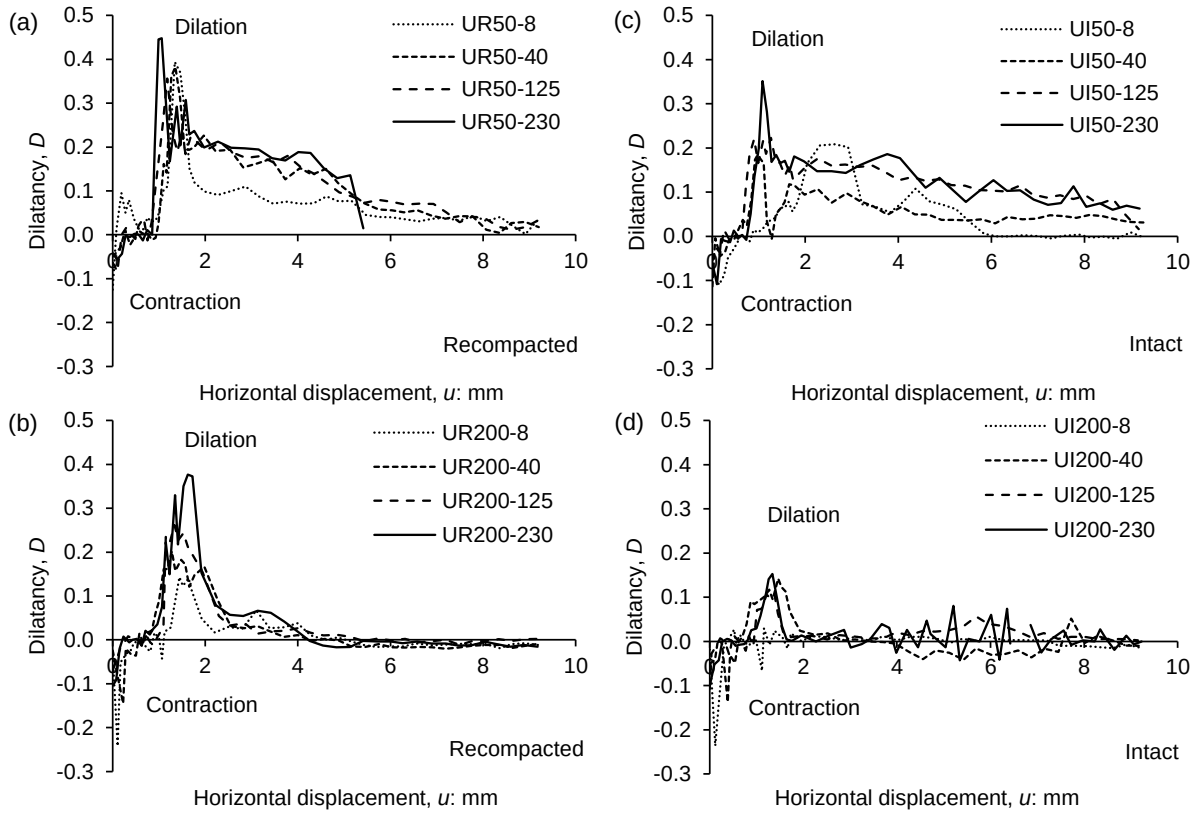

Fig. 12. Evolution of dilatancy with displacement for (a) & (b) recompacted loess and (c) & (d) intact loess

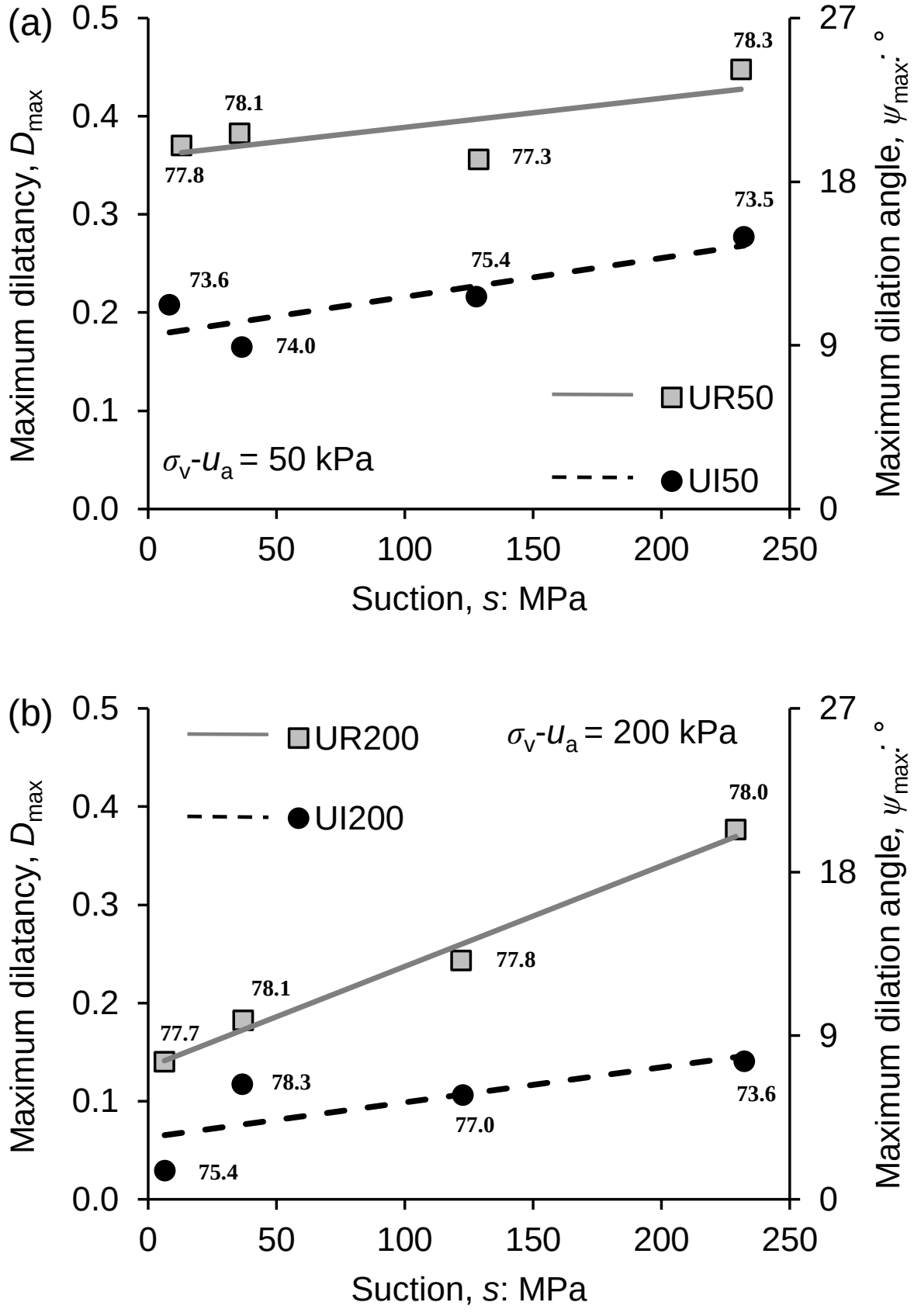

Fig. 13. Influence of suction and microstructure on maximum dilatancy under net stress of (a) 50 kPa and (b) 200 kPa

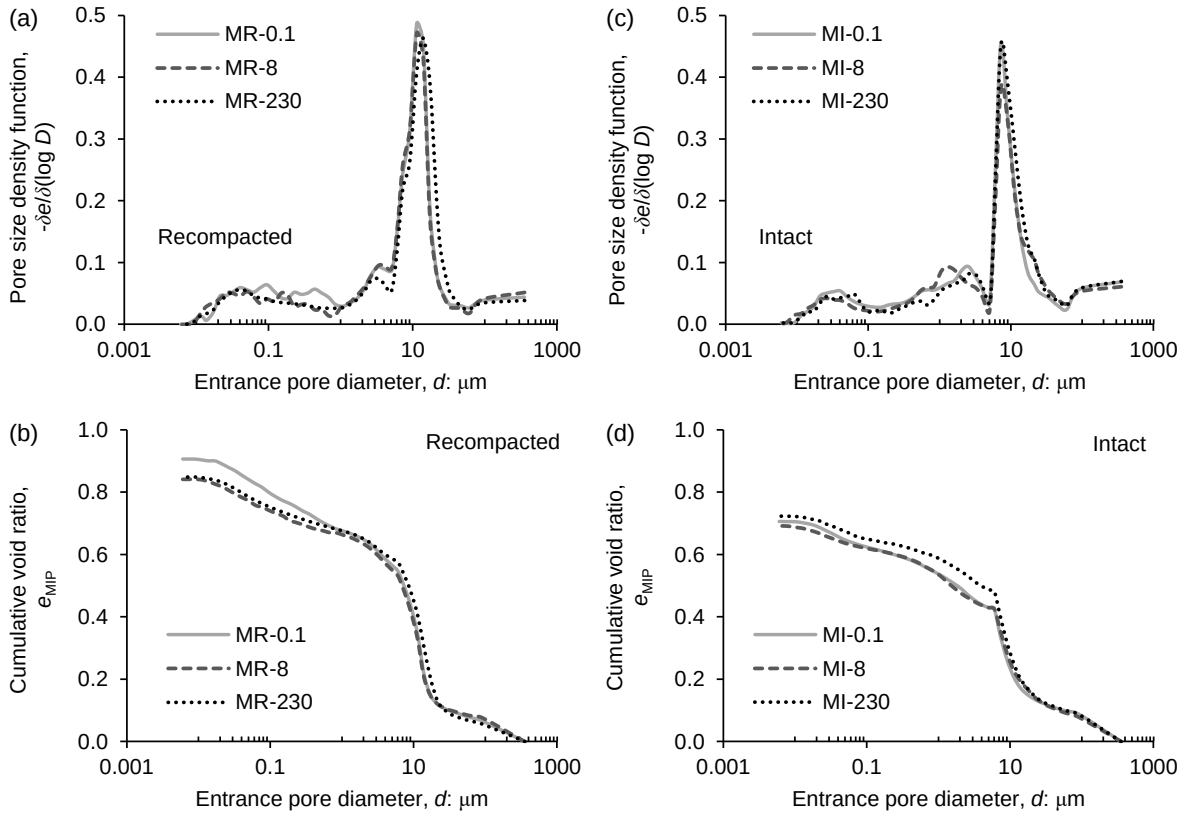

Fig. 14. MIP test results in terms of (a) & (c) pore size density functions and (b) & (d) cumulative void ratios for recompacted and intact loess

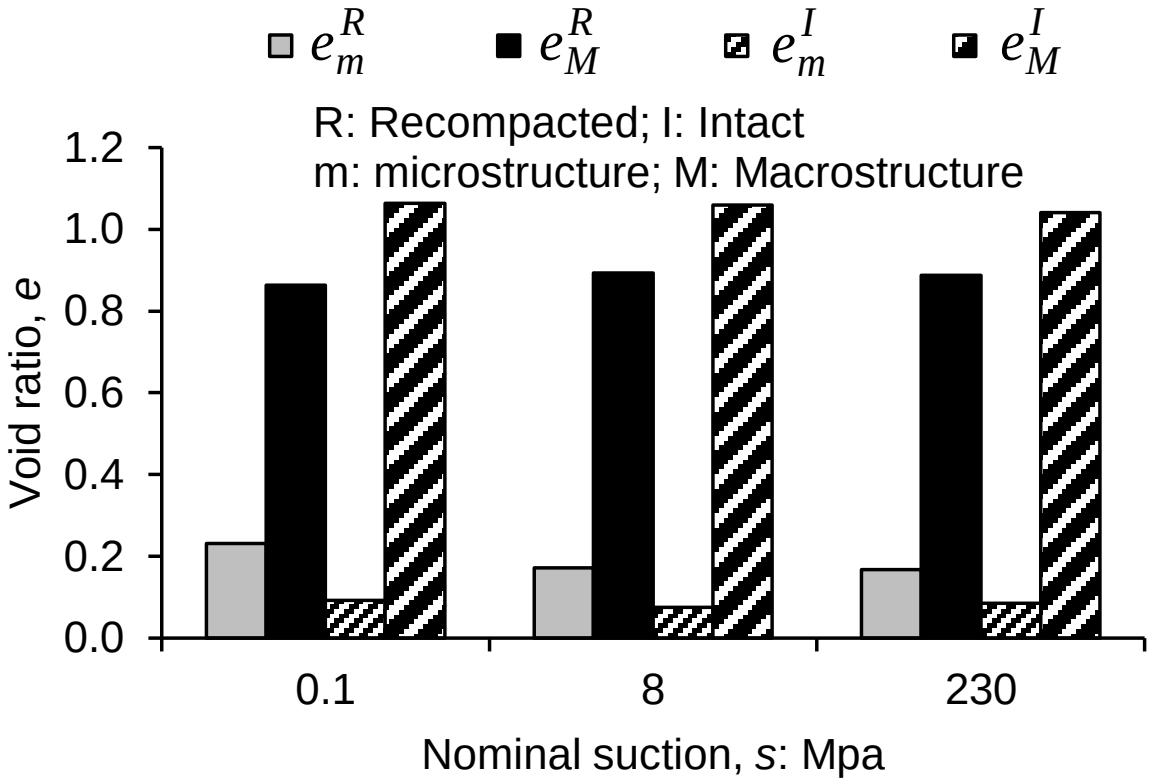

Fig. 15. Microvoid and macrovoid ratios of recompacted and intact loess at different suctions

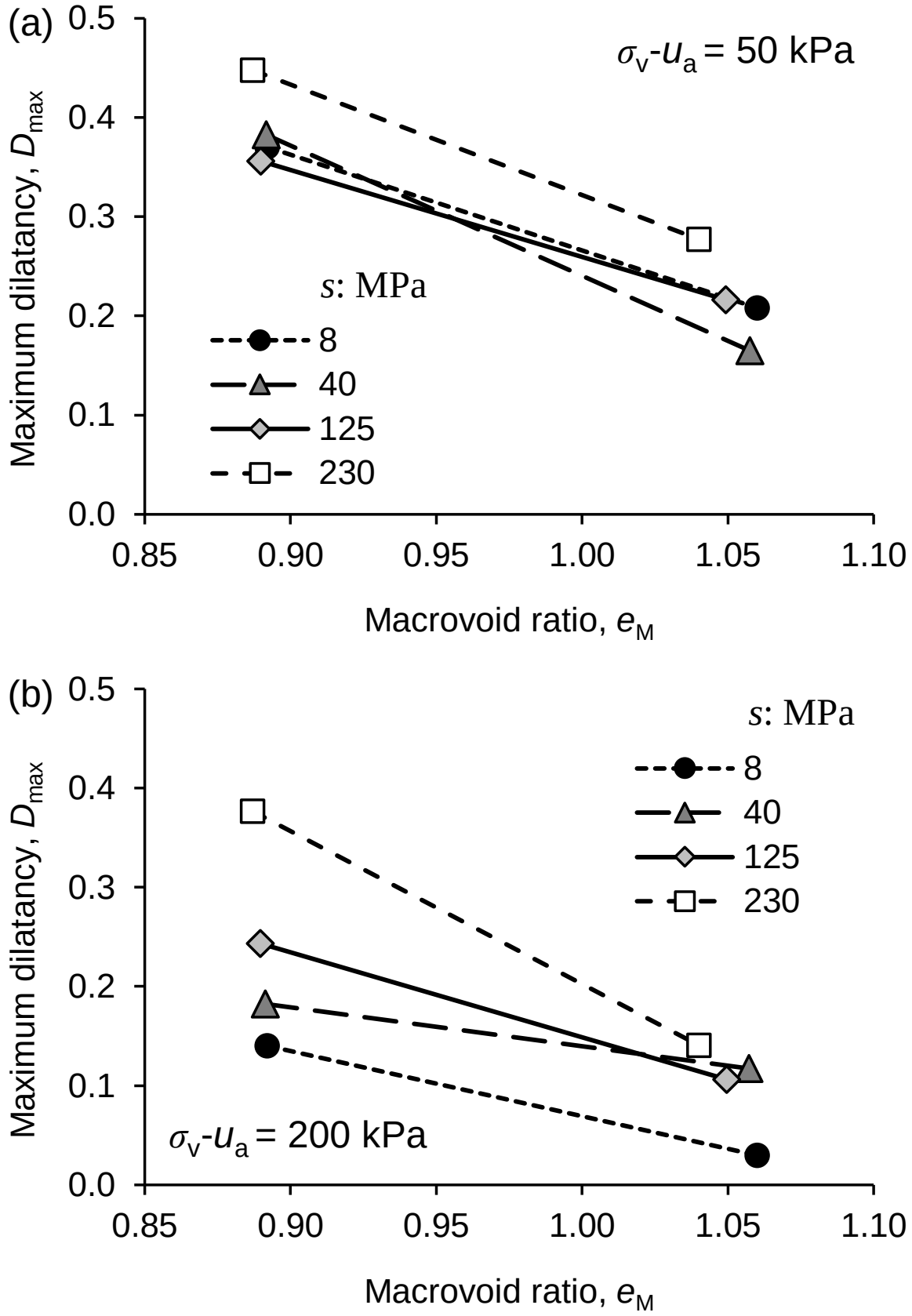

Fig. 16. Effects of macrovoid ratio on maximum dilatancy at net normal stress of (a) 50 kPa, and (b) 200 kPa

Table 1. Microstructural properties inferred from SWRCs of recompacted and intact loess

Specimen type	Microstructural degree of saturation S_r^m	Microstructural parameter ξ_m	Average void ratio e_{ave}	Microvoid ratio e_m	Macrovoid ratio e_M
Recompacted	0.30	0.30	1.06	0.32	0.74
Intact	0.18	0.18	1.14	0.21	0.93

Table 2. Details of the test programme and conditions of saturated tests

Test ID	Specimen type	Initial void ratio e_0	Initial degree of saturation S_{r0}	Vertical effective stress σ'_v (kPa)	Void ratio after compression e_c	Degree of saturation after compression S_{rc}
SR50		1.111	0.29	50.4	1.089	0.30
SR100	Recompacted	1.114	0.29	100.3	1.090	0.29
SR200		1.085	0.30	199.9	1.060	0.30
SI50		1.217	0.26	50.4	1.168	0.27
SI100	Intact	1.194	0.27	100.3	1.152	0.28
SI200		1.148	0.28	199.9	1.063	0.30

Table 3. Details of the test programme and conditions of unsaturated tests

Test ID	Specimen type	Initial void ratio e_0	Initial degree of saturation S_{r0}	Vertical net stress $\sigma_v - u_a$ (kPa)	Suction s (MPa)	Relative compaction RC (%)
UR50-8	Recompacted	1.090	0.29	50.4	13.0	77.8
UR50-40		1.091	0.29		35.6	78.1
UR50-125		1.103	0.30		128.9	77.3
UR50-230		1.092	0.29		231.1	78.3
UR200-8		1.108	0.31	199.9	6.4	77.7
UR200-40		1.095	0.29		37.1	78.1
UR200-125		1.094	0.29		121.9	77.8
UR200-230		1.092	0.29		228.9	78.0
UI50-8	Intact	1.247	0.27	50.4	8.4	73.6
UI50-40		1.211	0.30		36.6	74.0
UI50-125		1.159	0.28		128.0	75.4
UI50-230		1.214	0.26		232.1	73.5
UI200-8		1.142	0.33	199.9	6.5	75.4
UI200-40		1.087	0.39		36.7	78.3
UI200-125		1.118	0.30		122.7	77.0
UI200-230		1.206	0.26		232.2	73.6

Table 4. Summary of MIP test results on unsaturated recompacted, and intact loess

Test ID	Specimen type	Suction MPa	Delimiting pore diameter μm	d_M^* μm	d_m μm	e	e_{MIP}	e_{nd}	e_m	e_M
MR-0.1	Recompacted	0.06	1.059	11.338	0.096	1.094	0.906	0.188	0.231	0.863
MR-8		8	0.682	11.335	0.050	1.064	0.841	0.223	0.171	0.892
MR-230		230	0.841	13.947	0.040	1.055	0.849	0.206	0.168	0.887
MI-0.1	Intact	0.08	0.151	7.248	0.040	1.156	0.706	0.450	0.093	1.063
MI-8		8	0.121	7.248	0.026	1.135	0.692	0.444	0.076	1.060
MI-230		230	0.183	7.248	0.040	1.126	0.723	0.403	0.086	1.040

* $\boldsymbol{d_M}$: dominant macropore diameter; $\boldsymbol{d_m}$: dominant micropore diameter; $\boldsymbol{e}$: void ratio; $\boldsymbol{e_{MIP}}$: cumulative MIP void ratio; $\boldsymbol{e_{nd} = e - e_{MIP}}$: non-detected void ratio; $\boldsymbol{e_m}$: microvoid ratio; $\boldsymbol{e_M = e - e_m}$: macrovoid ratio.